Wiley
Structural Control and Health Monitoring
Volume 2024, Article ID 4204316, 23 pages
https://doi.org/10.1155/2024/4204316

WILEY

Research Article

A Bayesian Probabilistic Framework for Building Models for Structural Health Monitoring of Structures Subject to Environmental Variability

Patrick Simon,[1] **Ronald Schneider**,[1] **Matthias Baeßler**,[1] **and Guido Morgenthal**[2]

[1]*Bundesanstalt für Materialforschung und-prüfung (BAM), Berlin, 12205, Germany*
[2]*Professur Modellierung und Simulation-Konstruktion, Institut für Konstruktiven Ingenieurbau, Bauhaus-Universität Weimar, Weimar, 99423, Germany*

Correspondence should be addressed to Patrick Simon; patrick.simon@bam.de

Received 20 March 2024; Revised 3 June 2024; Accepted 10 June 2024

Academic Editor: Young-Jin Cha

Managing aging engineering structures requires damage identification, capacity reassessment, and prediction of remaining service life. Data from structural health monitoring (SHM) systems can be utilized to detect and characterize potential damage. However, environmental and operational variations impair the identification of damages from SHM data. Motivated by this, we introduce a Bayesian probabilistic framework for building models and identifying damage in monitored structures subject to environmental variability. The novelty of our work lies (a) in explicitly considering the effect of environmental influences and potential structural damages in the modeling to enable more accurate damage identification and (b) in proposing a methodological workflow for model-based structural health monitoring that leverages model class selection for model building and damage identification. The framework is applied to a progressively damaged reinforced concrete beam subject to temperature variations in a climate chamber. Based on deflections and inclinations measured during diagnostic load tests of the undamaged structure, the most appropriate modeling approach for describing the temperature-dependent behavior of the undamaged beam is identified. In the damaged state, damage is characterized based on the identified model parameters. The location and extent of the identified damage are consistent with the cracks observed in the laboratory. A numerical study with synthetic data is used to validate the parameter identification. The known true parameters lie within the 90% highest density intervals of the posterior distributions of the model parameters, suggesting that this approach is reliable for parameter identification. Our results indicate that the proposed framework can answer the question of damage identification under environmental variations. These findings show a way forward in integrating SHM data into the management of infrastructures.

1. Introduction

Bridges in road networks are exposed to ever-increasing heavy goods traffic. At the same time, numerous existing bridges were designed according to codes and standards that do not reflect the forecasted demands and/or current design principles. In addition, many bridges are subject to the effects of (advanced) deterioration. To support decisions on actions to be taken to ensure the required safety and performance, infrastructure managers are reassessing bridges with identified potential deficiencies [1].

If an initial structural assessment based on current codes and standards—possibly in conjunction with supplementary recommendations concerning the demand and capacity of existing bridges—fails to demonstrate compliance with safety and performance requirements, existing reassessment guidelines allow for the consideration of additional object-specific information in the structural assessment [2, 3]. This information can, for example, be derived from load/load effects monitoring, load tests, vibration measurements, and nondestructive testing (NDT). In case compliance with the prescribed requirements can still not be demonstrated,

infrastructure managers may still be able to safely operate structurally deficient bridges if they restrict traffic loads and/or employ global/local structural health monitoring (SHM) systems to inform near real-time decisions for avoiding catastrophic failures.

Such SHM systems are typically deployed to (a) identify potentially critical damages or deterioration processes, or (b) monitor the development of identified damages or deterioration processes. A special application is the identification of structural damages from structural response data (e.g., strains, deformations, and vibrations). To achieve this goal, it is generally accepted [4–7] that physics-based methods must be applied, in which structural models—typically finite element (FE) models—are updated with observed data.

There are several challenges in building structural models to infer the structural condition from SHM data through model updating:

(1) A structure can be modeled with different levels of sophistication regarding the applied mechanical theories (e.g., Euler–Bernoulli or Timoshenko beam theory, P-delta effects, and nonlinear material behavior), its representation in a finite element model (e.g., beam, shell, or solid elements), and the requirement of considering secondary/tertiary and/or nominally non-load-bearing members/components.

(2) In addition to the level of model sophistication, it is important to properly choose the model parameters, which are included in the model updating. Too few parameters may limit the model's ability to reflect the actual physical behavior, but too many parameters increase the model complexity and may lead to overfitting, in which case the parameters do not retain any physical meaning.

(3) Uncertainty in the parameters of a model, its capability to reflect the *true* physical phenomena, and the uncertainty in the observed data need to be addressed.

A major challenge in SHM is the influence of environmental and operational variability (EOV) on the structural behavior [4, 8–12]. Environmental variability includes, for example, variability in ambient temperatures, wind conditions, humidity, and sun exposure. Operational variability exists, for example, due to variable traffic loads on bridges, variable water levels in reservoirs, and variable storage loads on offshore platforms as well as variable operating conditions of structural systems (such as the opened/closed condition of drawbridges or variable directions/speeds of wind turbine rotors). For many structural systems including road bridges, the influence of variable environmental conditions on the temperature of the structural system is one of the most relevant influences because the system temperature affects the material properties of its components, its stress-strain/deformation state, and the behavior of its bearings.

When using model updating, there is a risk of incorrectly characterizing damages from SHM data or, more importantly, missing it altogether if the data are simply normalized in function of the environmental and operational conditions [4]. The inherent variability of structural parameters can be captured with probabilistic parametric models, which are a function of the environmental and operational influences. If there exist models on the nature of the influence, dependent structural parameters can be explicitly described by these models [13, 14]. As an alternative, a hierarchical probabilistic model of the relevant structural parameters with temperature-dependent mean functions has been applied in the literature, where the parameters of the mean function are included as additional hyperparameters in the hierarchical model [15]. More specifically, the existing works describe the effect of varying structural temperatures on material properties with the help of simplistic empirical models [13, 15]. This is a step forward towards solving the problem of identifying structural damages in real structural systems based on SHM data. However, to enhance the damage identification process and to enable a subsequent assessment of the structural performance, the influence of EOV should be described by physics-based models [4].

Motivated by this, we present a Bayesian probabilistic framework for building models for damage identification in structural systems subject to environmental variability. It includes a methodological workflow for model-based structural health monitoring, enables a quantitative evaluation of modeling choices, penalizes overfitting, and captures the governing parametric, model, and observation uncertainties. The framework accounts for the effect of varying environmental conditions on the structural behavior by explicitly modeling the dependence of structural parameters on environmental influences and thus enables a distinction between the effect of environmental influences and structural damages. The framework is consistent with the probabilistic and semiprobabilistic modeling and safety concepts encoded in modern structural codes and standards. Thus, the probabilistic diagnostic information obtained using the proposed approach can subsequently be incorporated into structural models suitable for assessing the safety and performance of monitored structural systems.

This paper is organized as follows: Section 2 presents the proposed framework for model building and damage identification. Section 3 applies the framework to a progressively damaged reinforced concrete beam subject to varying ambient temperatures in a climate chamber. The static response data forming the basis of the case study is measured in a series of diagnostic load tests. To validate the approach, an additional numerical study is presented in Section 4. Finally, Sections 5 and 6 discuss and conclude our contribution.

2. Methodology

2.1. Bayesian Probabilistic Framework for Model Building and Damage Identification

2.1.1. Stochastic Model Class. The main conceptual element of our proposed framework is the stochastic model class

originally introduced in [16]. We adopt this concept to formally address the issues related to identifying damage in structural systems subject to environmental variability. Within this context, a stochastic model class consists of the following:

(1) A set of parametrized, deterministic submodels of the underlying physical phenomena. This includes submodels of the mechanical behavior of the structure, the effect of EOV, and possible damages in terms of their location, type, and severity. The submodels are coupled to model the underlying fundamental physics of the system (see Section 2.2 for more details). Note that the submodels describing structural damages can be extended to represent time-dependent deterioration processes [13, 17, 18].

(2) A parametrized probabilistic model of the deviations between the observed data and the corresponding predictions of the deterministic system model (see Section 2.3). This bridging the gap between a deterministic system model and a probabilistic model is also known as "stochastic embedding" [16]. Based on the probabilistic model of the prediction errors and the deterministic model of the physical system, a likelihood function can be formulated to probabilistically describe the relation between the observed data and the parameters of the system model. The likelihood function describes the plausibility of the observed data conditional on a certain value of the parameters of the employed physical and probabilistic submodels.

(3) A joint probability distribution—the prior distribution—of all uncertain parameters of the physical and probabilistic submodels. This distribution reflects the relative plausibility of possible parameter values and their stochastic dependencies (see Section 2.3). It represents the prior knowledge or initial belief about the model parameters and is derived from all available information including, for example, engineering judgment and experience, design documents, codes, standards and guidelines [19], NDT, and material tests [20].

Within a stochastic model class, the posterior or updated knowledge of the uncertain model parameters in terms of their posterior distribution is obtained by combining the prior knowledge of the model parameters (described by their prior distribution) and the observed data (described by the likelihood function) by applying Bayes' rule (see Section 2.4). This process is commonly referred to as Bayesian inference, Bayesian system identification, Bayesian model updating, or Bayesian updating.

Competing stochastic model classes can be formulated to reflect different modeling approaches. Different model classes can include different deterministic submodels to describe the physics of the system. In addition, they can be based on different models of the model and observation uncertainty or include different prior distributions of the model parameters.

2.1.2. Methodological Workflow. Based on the concept of stochastic model classes, we define a series of methodological steps to formalize the process of building models of structural systems subject to environmental variability and identifying possible damages in such structures (see Figure 1).

The proposed workflow is divided into two main parts. The first part consists of several steps performed in a *reference phase* in which observed data from this phase are utilized to (a) learn the behavior of the undamaged structure subject to EOV within each defined stochastic model class and (b) select the *most plausible* stochastic model class based on these data [21, 22]. The most plausible class is subsequently extended with submodels representing possible damages. The second part of the workflow comprises a sequence of steps performed in a *monitoring phase,* in which the available data are then used to identify structural damages. The basic structure of this workflow reflects Axiom II of the fundamental Axioms of SHM [23], which states that the assessment of damage requires a comparison between two system states.

The individual steps in the proposed methodological workflow are as follows:

(1) We formulate a set of stochastic model classes to reflect the relevant competing hypotheses concerning the physical phenomena and the level of model sophistication, *without* submodels for damage. A thorough and transparent modeling approach calls for the explicit declaration of theories and assumptions prior to looking at any data.

(2) We perform Bayesian inference within all formulated stochastic model classes based on data from the reference phase to obtain updated models (see Section 2.4).

(3) We select the most plausible probabilistic model class with the help of model quality indicators, which are introduced in Section 2.5.

(4) We quantify the parametric and prediction uncertainty, and the prediction errors introduced in Section 2.3 conditional on the observed data.

(5) For the monitoring phase, we extend the most plausible probabilistic model class by adding one or more submodels for possible damages. In this way, a new set of competing stochastic model classes is defined to reflect all relevant hypotheses regarding possible damages.

(6) Optionally, we optimize the monitoring setup for the monitoring phase to enhance the damage identification process. For example, the sensor placement can be refined or other types of sensors selected based on maximizing the information gain or the value of information [24, 25]. Consequently, the monitoring system employed in the monitoring phase can be different from the monitoring system applied in the reference phase.

(7) We perform Bayesian inference within the stochastic model classes *with* and *without* submodels for

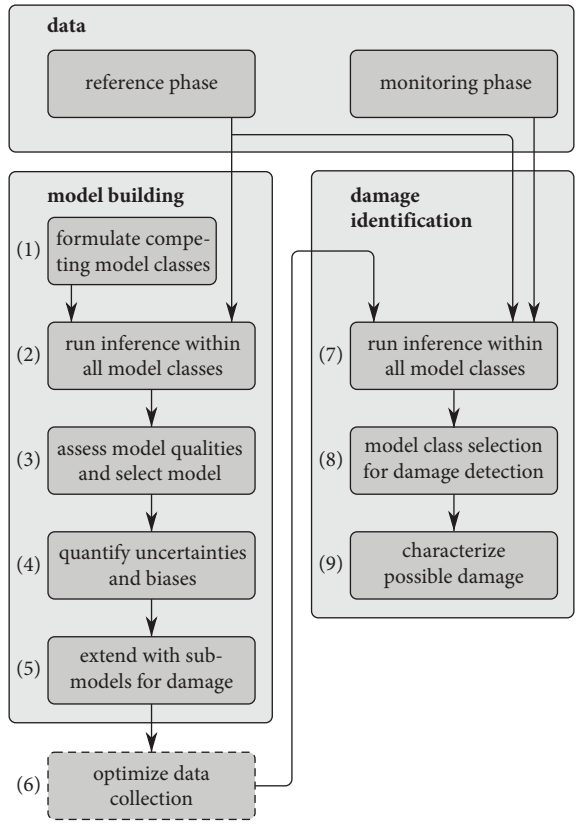

FIGURE 1: Proposed workflow of methodological steps involved in building models of structural systems subject to EOV in a reference phase and identifying structural damage in a monitoring phase.

damage based on data from the monitoring phase, considering the information from the reference phase. There are two possible approaches to account for the information from the reference phase: either deterministically fix (some of) the parameters inferred in the reference phase, for example, at their most probable values [13], or perform sequential Bayesian updating with the data from the reference and monitoring phase [26].

(8) Based on model quality indicators, we determine whether the undamaged probabilistic model class or one of the classes including damage is more plausible.

(9) If damage appears to be present, we characterize the damage based on the posterior distribution of the corresponding parameters of the damage models.

2.2. Generic Deterministic System Model. A key component of a stochastic model class described in Section 2.1.1 is the parameterized deterministic model of the structural system subject to EOV and damage. A generic representation of this model is shown in Figure 2. It consists of several coupled submodels including a set of submodels $\{q_{E,1}(y,\theta_E),\ldots, q_{E,N_E}(y,\theta_E)\}$ describing the effect of EOV on the parametres of the structural model, a set of submodels $\{q_{D,1}(y,\theta_D),\ldots,q_{D,N_D}(y,\theta_D)\}$ representing possible structural damages, and a submodel $q_S(y,\theta_S,q_{E,1}\ (y,\theta_E),\ldots,\ q_{E,N_E}(y,\theta_E),q_{D,1}(y,\theta_D),\ldots,q_{D,N_D}(y,\theta_D))$ describing the structural response as a function of the effect of EOV and possible structural damages. In the following, we write $q(y,\theta_p)$ to designate the overall system model to simplify the notation. In this generic representation, y are the actions on the system (input) and $\theta_P = [\theta_E^T,\theta_D^T,\theta_S^T]^T$ are the parameters of the coupled submodels. The model parameters and input influence the response of the structure and thus the model output. Within the scope of this contribution, it is assumed that the input relevant for the model building and damage identification is observed and free from any observation uncertainty, i.e., the exact value of the input y is assumed to be known. Note that this is not a limitation, as the proposed framework can be extended to account for uncertainty in y.

2.3. Uncertainty Quantification. To use model updating as the basis for identifying damage in structural systems, it is desirable to identify and quantify the governing sources of uncertainty. In this contribution, uncertainty quantification is understood to comprise three steps: (a) classify uncertainties according to their sources, (b) model the uncertainties using probability theory, and (c) describe them.

Based on categorizations from the literature [27, 28], we distinguish between the following sources of uncertainty:

(i) *Model uncertainty*—often also referred to as *model form error, model structure uncertainty,* or *model inadequacy*—is the discrepancy between the model predictions and the *true* physical behavior.

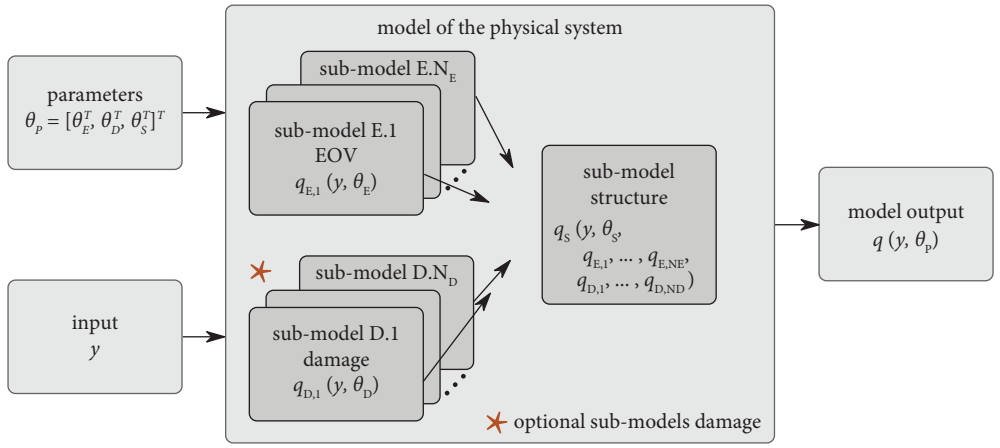

FIGURE 2: Generic representation of the deterministic model of a structure subject to EOV and damage. It consists of submodels describing the effect of EOV, submodels representing possible damages, and a submodel describing the structural response. The individual submodels are coupled to describe the overall system behavior.

(ii) O*bservation uncertainty* is the difference between the *true* system behavior and the observed system behavior. The observed system behavior can, for example, be measurements or processed data derived from measurements.

(iii) *Parameter uncertainty* is the uncertainty in the parameters of all physical submodels of a probabilistic model class.

Parameter uncertainty is captured by modeling the model parameters θ_p as (correlated) random variables. With regard to model and observation uncertainties, there are various ways of probabilistically modeling these uncertainties [27–29]. They can, for example, be described by introducing additional parameters that are added to or multiplied with q and subsequently modeled as (correlated) random variables. As an illustrative example, consider the following commonly applied additive model [28]:

$$z_i = q\left(y_i, \theta_p\right) + \delta_i + \varepsilon_i. \tag{1}$$

In this formulation, the i^{th} observation z_i of the system response which corresponds to input y_i is predicted as the sum of the model output $q(y_i, \theta_p)$ and two additional parameters δ_i and ε_i, where δ_i is the difference between the *model predicted* and *true* system response and ε_i is the difference between the *true* and *observed* system response. As the actual values of δ_i and ε_i are unknown, they are also modeled as random variables (in addition to the model parameters θ_p).

Probabilistic models of the type defined in equation (1) are commonly referred to as *data prediction models*, e.g., [30]. Such models serve two purposes: (i) by modeling the parameter, model, and observation uncertainties probabilistically and propagating them through such a data prediction model, a probabilistic description of the predicted observations is obtained. In this way, the *prediction uncertainties* are quantified. (ii) Based on the mathematical relations encoded in the data prediction model and the probabilistic model of the model and observation uncertainties, a likelihood function can be formulated, which probabilistically relates the observation of the system response with the model parameters [28, 29, 31] (see also Section 2.4). This function forms the basis for learning the probability distribution of the model parameters from the observed data using Bayesian model updating (see Section 2.4). Since the model and observation uncertainties are included in the data prediction model as additional random variables, their probability distributions can also be learned from the data.

Note that the model in equation (1) describes the model uncertainty at the system level through the additional uncertain parameter δ_i. A similar approach can be applied to quantify model uncertainties at the level of the submodels. In addition, it should be noted that the model and observation uncertainties are in the literature often jointly modeled at the system level by a *prediction error* representing the overall difference between the *model-predicted* and *observed* system response [16, 21, 28, 29]. We also apply this approach in the case study in Section 3. Finally, note that the proposed framework provides the means for defining competing models of the model and observation uncertainties within competing stochastic model classes [29]. In this way, the most appropriate model of these uncertainties can be identified from the observed data jointly with the most plausible model of the physical system.

2.4. Bayesian Model Updating. A large body of the literature on updating structural models (mostly finite element models) based on experimental data has emerged over the past decades. An overview can, for example, be found in [1, 32]. According to [32], the prevalent approaches can be classified into three categories: deterministic optimization methods (i.e., residual minimization techniques), Bayesian methods, and error domain model falsification.

In this contribution, we adopt Bayesian methods for two reasons: (1) in a Bayesian approach, the prior knowledge of the structural system and the monitoring process including

the associated uncertainties are explicitly quantified in terms of the deterministic physics-based model, the data prediction model, and the prior distribution of the model parameters. These are, for example, derived based on codes and standards, engineering judgment, expert knowledge, previous measurements, and tests as well as equipment certificates. When new data become available, Bayesian analysis is performed to update the probabilistic distribution of the model parameters systematically and consistently. Importantly, Bayesian methods can solve—in addition to globally identifiable inverse problems—locally identifiable problems with multiple possible solutions [33]. (2) Modern performance-based codes and standards [34, 35] also quantify uncertainties based on probability theory. The probabilistic diagnostic information resulting from Bayesian model updating can, therefore, be consistently included in code-based assessments of structural systems, for example, in terms of characteristic values.

In the following, Bayesian model updating is briefly described. As a starting point, we consider the following data prediction model, which predicts the i^{th} observation z_i of the system response as a function of the input y_i:

$$z_i = q\left(y_i, \theta_p\right) + \varepsilon_i. \tag{2}$$

In this model, an overall prediction error $\varepsilon_i = z_i - q(y_i, \theta_p)$ is introduced to jointly represent the model and observation uncertainty (see also Section 2.3). The vector-valued prediction error ε_i is here assumed to follow a multivariate Gaussian distribution with zero mean and covariance matrix $\Sigma_\varepsilon(\theta_\varepsilon)$ with uncertain parameters θ_ε, i.e., $\varepsilon_i \sim \mathcal{N}(\varepsilon_i; 0, \Sigma_\varepsilon(\theta_\varepsilon))$. Subsequently, all uncertain parameters of the problem are collected in the overall parameter vector $\theta = [\theta_p^T, \theta_\varepsilon^T]^T$ and the *prior* distribution $p(\theta)$ of θ is assigned based on the available knowledge.

Now, let $\mathcal{D}_i = \{\hat{z}_i, \hat{y}_i\}$ denote the i^{th} *dataset*, where $\hat{z}_i$ is a vector of n_d observation of the system response and $\hat{y}_i$ are the corresponding observations of the input. Based on the data prediction model and the probability density function of the prediction error, the likelihood function $L(\theta \mid \mathcal{D}_i) \propto p(\mathcal{D}_i \mid \theta)$ describing the plausibility of observing $\mathcal{D}_i$ given a certain realization of the model parameters θ can be formulated. It corresponds here to the probability density of $\hat{z}_i$ conditional on $\hat{y}_i$ and θ, which is equal to the probability density of ε_i taking the value $\hat{z}_i - q(\hat{y}_i, \theta_p)$, i.e.,

$$\begin{aligned} L(\theta \mid \mathcal{D}_i) &= \mathcal{N}\left(\hat{z}_i - q\left(\hat{y}_i, \theta_p\right); 0, \Sigma_\varepsilon\left(\theta_\varepsilon\right)\right) \\ &= \frac{\exp\left[-J\left(\theta, \mathcal{D}_i\right)\right]}{\sqrt{(2\pi)^{n_d} \det\left(\Sigma_\varepsilon\left(\theta_\varepsilon\right)\right)}}, \end{aligned} \tag{3}$$

with

$$J\left(\theta, \mathcal{D}_i\right) = \frac{1}{2}\left[\hat{z}_i - q\left(\hat{y}_i, \theta_p\right)\right]^T \sum_{\varepsilon}^{-1}\left(\theta_\varepsilon\right)\left[\hat{z}_i - q\left(\hat{y}_i, \theta_p\right)\right], \tag{4}$$

where $J(\theta, \mathcal{D}_i)$ is commonly referred to as the *measure-of-fit function* [21, 36] of the i^{th} dataset $\mathcal{D}_i$.

Different prediction errors $\varepsilon_1, \ldots, \varepsilon_{n_o}$ corresponding to n_o and different datasets $\mathcal{D}_1, \ldots, \mathcal{D}_{n_o}$ are modeled as independent and identically distributed, conditional on a certain realization of the hyper parameters θ_ε. Based on this hierarchical model, the likelihood function describing *all* available data $\mathcal{D} = \{\mathcal{D}_i\}_{i=1}^{n_o}$ is simply the product of the likelihood functions describing the individual observations:

$$L(\theta \mid \mathcal{D}) = \prod_{i=1}^{n_o} L\left(\theta \mid \mathcal{D}_i\right). \tag{5}$$

The available data $\mathcal{D}$ and the prior knowledge on the uncertain parameters θ can now be combined by applying Bayes' rule, which updates the prior distribution $p(\theta)$ with data $\mathcal{D}$ to the *posterior* distribution $p(\theta \mid \mathcal{D})$:

$$p(\theta \mid \mathcal{D}) = \frac{L(\theta \mid \mathcal{D})\, p(\theta)}{\int_\theta L(\theta \mid \mathcal{D})\, p(\theta)\, \mathrm{d}\theta} = c_E^{-1}\, L(\theta \mid \mathcal{D})\, p(\theta), \tag{6}$$

where c_E is the *evidence* of the stochastic model class [16], which is proportional to the probability density of data $\mathcal{D}$, i.e., $c_E \propto p(\mathcal{D})$.

In most cases, $p(\theta \mid \mathcal{D})$ cannot be determined analytically. Instead, samples from $p(\theta \mid \mathcal{D})$ must be generated numerically. To this end, we apply the adaptive version of Bayesian updating with structural reliability methods (aBUS) [36], which provides an approximation of the evidence c_E as a by-product.

Figure 3 illustrates Bayesian model updating based on a single dataset $\mathcal{D}_i$.

2.5. Indicators of Model Quality. Indicators of model quality cannot be used to assess the *absolute* quality of a stochastic model class but can only be utilized to compare different stochastic model classes *relative* to each other. It is thus necessary to postulate a set of competing probabilistic model classes.

All models that are updated with observed data bear the danger of overfitting, i.e., with a growing number of parameters considered in the model updating the model seems to *fit* the data better, but instead of representing the underlying physics, the model parameters compensate the existing model and observation uncertainty. Several quantitative measures have emerged, which reward stochastic model classes for fitting the data while at the same time penalizing properties that could lead to overfitting. They are presented in the following sections.

2.5.1. Akaike Information Criterion. The Akaike information criterion (AIC) was developed in [37] as

$$\mathrm{AIC} = 2k - 2\ln(\hat{L}), \tag{7}$$

where k is the number of parameters and $\hat{L}$ is the value of the likelihood function at the most probable value (MPV) of the parameters θ. In this way, this indicator is also available for methods that yield only a point estimate of the parameters, such as the maximum likelihood method.

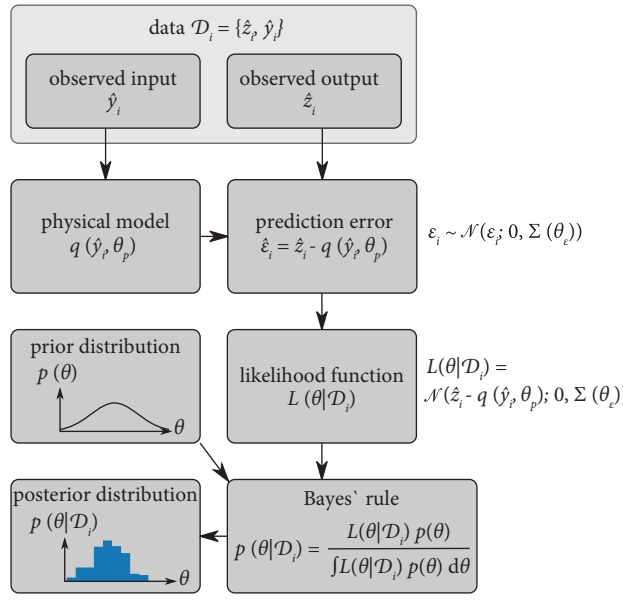

FIGURE 3: Illustration of the Bayesian model updating based on a single dataset. The prediction error is the difference between the model-predicted and observed system response, conditional on the observed input. Based on the probabilistic error model, a likelihood function is formulated to link the data with the model parameters. This function is combined with the prior distribution of the parameters using Bayes' rule to determine the posterior distribution of the parameters.

The AIC is no absolute measure but enables a comparison of different model classes, whereby the model with the lowest AIC is the most appropriate. It should be highlighted that the AIC is a logarithmic measure.

The AIC can be rescaled after [16]:

$$\mathrm{AIC}^* = \ln(\hat{L}) - k, \tag{8}$$

to facilitate a comparison with the evidence c_E or the model selection factor MSF (see Section 2.5.3).

This changes the sign, meaning the higher the AIC*, the better. It now resembles the *optimal data-fit minus the number of parameters.*

2.5.2. Bayesian Information Criterion. A metric similar to the AIC is the Bayesian information criterion (BIC), which was introduced in [38] as

$$\mathrm{BIC} = k \quad \ln(n) - 2\ln(\hat{L}), \tag{9}$$

where additionally the number of observations n is considered.

Like the AIC, it can be rescaled as [16]

$$\mathrm{BIC}^* = \ln(\hat{L}) - \frac{k}{2}\ln(n), \tag{10}$$

and now represents the *optimal data-fit minus the number of parameters divided by 2 times the logarithm of the number of observations.*

2.5.3. Bayesian Model Class Selection. Let $\mathcal{M} = \{M_1, \ldots, M_m\}$ be a set of m competing stochastic model classes, where each stochastic model class $M_i \in \mathcal{M}$ encodes the knowledge and assumptions required to formulate the likelihood function $L(\theta \mid \mathcal{D}, M_i)$ and prior distribution $p(\theta \mid M_i)$. By conditioning on M_i in the following, we explicitly indicate dependence on the encoded knowledge and assumptions.

For each stochastic model class M_i, the evidence $c_{E|M_i}$ can be computed as (see also equation (6))

$$c_{E|M_i} \propto p(\mathcal{D} \mid M_i) = \int_\theta L(\theta \mid \mathcal{D}, M_i)\, p(\theta \mid M_i)\, \mathrm{d}\theta. \tag{11}$$

If $\int_{\mathcal{D}} L(\theta \mid \mathcal{D}, M_i)\mathrm{d}\mathcal{D} = 1$ or equivalently $L(\theta \mid \mathcal{D}, M_i) = p(\mathcal{D} \mid \theta, M_i)$, it follows that the model evidence $c_{E|M_i}$ is equal to $p(\mathcal{D} \mid M_i)$. Note that the likelihood functions defined in equations (5) and (6) fulfill this condition.

According to [16], $p(\mathcal{D} \mid M_i)$ can be transformed to express the *average data-fit minus information gain.*

$$\ln[p(\mathcal{D} \mid M_i)] = E_{\theta|\mathcal{D},M_i}[\ln(p(\mathcal{D} \mid \theta, M_i))] - \mathrm{E}_{\theta|\mathcal{D},M_i}\left[\ln\frac{p(\theta \mid \mathcal{D}, M_i)}{p(\theta \mid M_i)}\right], \tag{12}$$

in which the expectation is determined with respect to the posterior distribution $p(\theta \mid \mathcal{D}, M_i)$. The second term in (12) corresponds to the *Kullback–Leibler divergence* [39].

Each of the model classes $M_i \in \mathcal{M}$ is assigned a *prior* probability $\Pr(M_i)$ to quantify the initial belief about their plausibility, where $\sum_i \Pr(M_i) = 1$. Based on the evidence $c_{E|M_i,\mathcal{M}} = p(\mathcal{D} \mid M_i)$, the *posterior* probabilities $\Pr(M_i \mid \mathcal{D})$ of each model class *after* observing the data $\mathcal{D}$ are inferred by applying Bayes' rule anew [16, 21, 22, 40]:

$$\Pr(M_i \mid \mathscr{D}) = \frac{p(\mathscr{D} \mid M_i)\Pr(M_i)}{\sum_i p(\mathscr{D} \mid M_i)\Pr(M_i)}. \tag{13}$$

If there is no prior knowledge on the relative plausibility of the m competing model classes, their *prior* probabilities can be assumed to be equal, i.e., $\Pr(M_i) = 1/m$. If this noninformative prior is utilized, the posterior probability $\Pr(M_i \mid \mathscr{D})$ emerging from (13) is also referred to as model selection factor (MSF) [41]:

$$\mathrm{MSF}_{\mathbf{i}} = \Pr(M_i \mid \mathscr{D}) = \frac{p(\mathscr{D} \mid M_i)}{\sum_i p(\mathscr{D} \mid M_i)}. \tag{14}$$

The MSF explicitly includes all competing model classes and quantifies their relative plausibility.

2.6. Damage Identification. The goal of damage identification is to (1) *detect* and (2) *characterize* possible damage in terms of location, type, and severity [23]. This corresponds to steps (8) and (9) of the proposed workflow in Section 2.1.2.

As a first step in damage detection, a single stochastic model class M_0 is chosen, which best represents the structure in the reference phase. This model class is then extended to represent the possibly damaged structural system in the monitoring phase. To this end, probabilistic parameterized submodels of damage may be assigned to each potentially damaged structural component within one stochastic model class M_1, e.g., [15] or different stochastic model classes $M_1, \ldots, M_n$ may be proposed to model different potential damage scenarios, e.g., [21].

Then, model quality indicators including the evidence $p(\mathscr{D} \mid M_i)$ are determined for each stochastic model class $M_i \in \{M_0, \ldots, M_n\}$, conditional on the data from the reference and monitoring phase. Finally, the posterior odds (the posterior ratio of relative plausibility) in favor of each stochastic model class representing the damaged structure $M_i \in \{M_1, \ldots, M_n\}$, $\Pr(M_i \mid \mathscr{D})/\Pr(M_0 \mid \mathscr{D})$, is computed as [42, 43]

$$\underbrace{\frac{\Pr(M_i \mid \mathscr{D})}{\Pr(M_0 \mid \mathscr{D})}}_{\text{posterior odds}} = \underbrace{\frac{p(\mathscr{D} \mid M_i)}{p(\mathscr{D} \mid M_0)}}_{\text{Bayes factor } BF_i} \times \underbrace{\frac{\Pr(M_i)}{\Pr(M_0)}}_{\text{prior odds}}, \tag{15}$$

where $\Pr(M_i)/\Pr(M_0)$ is the prior odds in favor of each damaged model class $M_i \in \{M_1, \ldots, M_n\}$ and $p(\mathscr{D} \mid M_i)/p(\mathscr{D} \mid M_0)$ is the Bayes factor BF_i. Note that (15) is only a reformulation of the model class selection presented in Section 2.5.3.

With the help of the Bayes factor BF_i, each stochastic model class representing the damaged structure $M_i \in \{M_1, \ldots, M_n\}$ can be compared to the stochastic model class representing the undamaged structure M_0 solely based on the data, independently of the prior belief. Damage detection based on the Bayes factor is thus explicitly separated from the prior judgment of the user, who can then adjust her belief about the health status of the structure.

The Bayes factor BF_i assesses the strength of evidence provided by the data in supporting the likelihood that the analyzed structure is indeed damaged, as opposed to being undamaged. A common interpretation of the magnitude of the Bayes factor was proposed by Jeffreys (see, e.g., Table 1 of [29]), where $\mathrm{BF}_i \geq 10$ is regarded as *strong* and $\mathrm{BF}_i \geq 100$ as *decisive* evidence.

In the special case, where the prior probabilities of all stochastic model classes $\Pr(M_i)$ are assumed to be equal, the Bayes factor becomes the ratio of the model selection factors. We will apply this approach in the remainder of this contribution.

To characterize damage conditional on the available data, the posterior distributions of the uncertain parameters of the damage models are examined. Damage characterization is, therefore, included in the parameter identification.

3. Case Study

In the current contribution, a simply supported reinforced concrete (RC) beam serves as a model of a bridge subject to environmental variations and damage. The case study does not include operational variations, and environmental variations are limited to variations in the ambient temperatures. As an additional limitation, the case study only considers the effect of varying ambient temperatures on the mechanical properties of the concrete material. This limitation excludes the effects of varying temperatures on other members, such as the bearings, for example.

The RC beam is subject to varying ambient temperatures in a climate chamber. In addition, it is progressively damaged in two consecutive three-point bending tests. In analogy to diagnostic load tests of bridges, the static response of the undamaged and damaged beam is measured in a series of load tests at the prescribed temperatures.

The case study has two main objectives:

(1) We implement the proposed framework for model building based on data obtained in the undamaged (reference) state. This includes a quantitative assessment of the quality of the proposed models and a quantification of the governing uncertainties conditional on the load test data.

(2) We evaluate the capabilities of *damage characterization*, i.e., we identify the location and severity of damage. This is achieved by comparing the posterior marginal distributions of the model parameters describing the damage to the damage observed in the real structural system.

The case study starts out by describing the experimental setup and diagnostic load tests in Sections 3.1 and 3.2. The model building is then presented in Sections 3.3 to 3.5. Finally, the damage characterization is described in Section 3.6.

3.1. Experimental Setup. The RC beam is 2.96 m long and has a 40 cm wide and 20 cm high cross section (see Figure 4). It consists of reference concrete C (0.45) [44], and Young's modulus of the concrete is 33.3 GPa [45]. The beam is reinforced with two steel rebars with 16 mm diameter as shown in Figure 4. In the climate chamber, the beam is

placed on a substructure such that it is simply supported with a span of 2.72 m (see Figure 4). The experimental setup is shown in Figure 5.

Three different states of the beam are considered:

(1) The *uncracked* beam in the initial (reference) condition.

(2) The *cracked_1* state, which resulted from an initial three-point bending test with a maximum load of 20 kN. The test led to the formation of the first cracks.

(3) The *cracked_2* state, which occurred after applying a maximum load of 28 kN in a second three-point bending test. The applied load corresponds to the ultimate load capacity of the beam.

3.2. Diagnostic Load Tests. A trolley with suspended weights shown in Figure 5 serves as a moveable vertical point load. The resulting point load of 3 kN is placed at three predetermined positions, as indicated on the left-hand side of Figure 6. In each load position, displacements and inclinations of the beam are measured for 1 minute with three displacement sensors (W1, W2, and W3) positioned at the quarter points of the beam and two inclination sensors (N1 and N2) located at the supports of the beam. The sensor setup is also shown at the top of Figure 6.

The data were averaged over the measured time, and the mean values of the displacements and inclinations were applied in the model building and damage diagnosis.

For each state of the beam, load tests are conducted at −25°C, −5°C, 5°C, 25°C, and 40°C. Before the static response of the beam is measured, it is ensured that the beam reaches a stationary temperature field within bounds of ±1 K. This condition is verified with two temperature sensors located inside the beam. In each test series, the first test of the series yielded implausible data and thus was identified as an outlier and removed.

Figure 6 presents the postprocessed data obtained during the different load tests.

3.3. Proposed Deterministic and Probabilistic Submodels. As a basis of the model building and damage identification, we consider several different deterministic and probabilistic submodels from which we construct different stochastic model classes of the RC beam. Each class contains a deterministic system model of the beam consisting of deterministic submodels describing (a) the effect of the beam temperature on the concrete material properties, (b) the damage induced by the three-point bending tests, and (c) the deformation response of the beam subject to the point load. The deterministic system model is illustrated in Figure 7.

The deterministic system model $q(y, \theta_p)$ predicts the rotations and deflections of the beam at the locations of the sensors W1, W2, W3, N1, and N2 as a function of the parameters θ_p and the input $y = [x_F, F, T]^T$, where F is the point load, x_F is the load position, and T is the beam temperature:

$$q\left(y, \theta_p\right) = [W1, W2, W3, N1, N2]^T. \tag{16}$$

In the following, the considered variants of the submodels of the deterministic system model, the probabilistic model of the model and observation uncertainties, the likelihood function derived on their basis, and the prior probabilistic model of the model parameters are presented.

3.3.1. Deterministic Submodels of the Structure. The deformation response of the beam subject to a point load is described by a linear-elastic FE model in the open-source framework OpenSEES [46, 47]. Two competing approaches are taken: the beam is modeled according to (a) classical Euler–Bernoulli beam theory and (b) Timoshenko beam theory, which includes shear deformation. A close spacing of the nodes of 1 cm is chosen. The only parameter of the Euler–Bernoulli beam model is the bending stiffness EI, where E is Young's modulus and I is the area moment of inertia. The latter is considered constant with a value of 26667 cm^4. The Timoshenko beam model includes Poisson's ratio ν_c as an additional parameter.

Figure 8 shows the FE model of the beam together with an illustration of both competing beam theories and the submodel for the cracked region. The flexural cracks in the RC beam resulting from the three-point bending test are not modeled explicitly, but their effect is implicitly integrated into the bending stiffness at the cross-sectional level. The damage model is discussed in more detail in Section 3.3.3.

3.3.2. Deterministic Submodel of the Temperature Effect. The laboratory experiment is designed such that the temperature variations only affect the mechanical properties of the RC beam. The relevant temperature-dependent material property of concrete is Young's modulus E. As described in the literature [34, 48–50], this property changes linearly with temperature.

Possible damage is modeled as a reduction of the bending stiffness EI (see Section 3.3.3), and the area moment of inertia I of the RC section in the uncracked state is considered constant (see Section 3.3.1). Therefore, the temperature-dependent bending stiffness EI is the only parameter that the EOV submodel provides as input to the submodel of the structure and can be modeled as a linear function of the beam temperature T:

$$\mathrm{EI}(T) = \mathrm{EI}_0 + \alpha T, \tag{17}$$

where EI_0 is the bending stiffness at 0°C and α is the temperature sensitivity of the bending stiffness.

3.3.3. Deterministic Submodel of Damage. A three-point bending test produces approximately uniformly spaced flexural cracks symmetrically distributed around the midspan of the beam. As indicated in Figure 8, the location and extent of the cracked region are defined by the distance x_D from the bearings. The reduction of the bending stiffness EI in the cracked region is modeled by the reduction factor D, i.e., the bending stiffness in this region is $D \times \mathrm{EI}(T)$. In this way, both the location and severity of the damage induced by the three-point bending test are quantified (the "classic" higher levels of damage identification [23]).

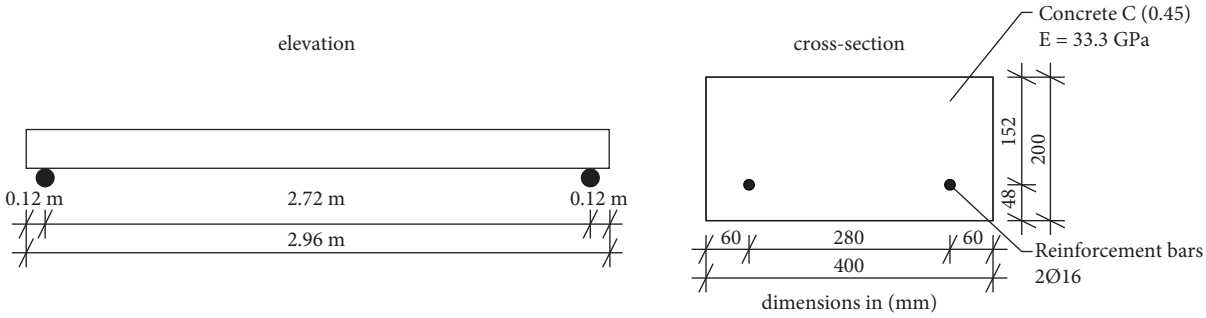

Figure 4: Elevation and cross section of the concrete beam.

Figure 5: RC beam inside the climate chamber together with the substructure and moveable trolley with suspended weights.

Damage is captured in the FE model by assigning the reduced bending stiffness of $D \times \mathrm{EI}(T)$ to all FE elements that are within the cracked region, i.e.,

$$\mathrm{EI}_{\mathrm{FEM},i} = \begin{cases} D \times \mathrm{EI}(T) & \text{if } x_D \le x_{1,i} \le l - x_D \wedge x_D \le x_{2,i} \le l - x_D, \\ \mathrm{EI}(T) & \text{else,} \end{cases} \tag{18}$$

where $\mathrm{EI}_{\mathrm{FEM},i}$ is the bending stiffness of the ith beam element and $x_{1,i}$ and $x_{2,i}$ are the coordinates of the corresponding start and end node.

3.3.4. Probabilistic Submodel of Model and Observation Uncertainty. In the present case study, model and observation uncertainties associated with the ith observation are

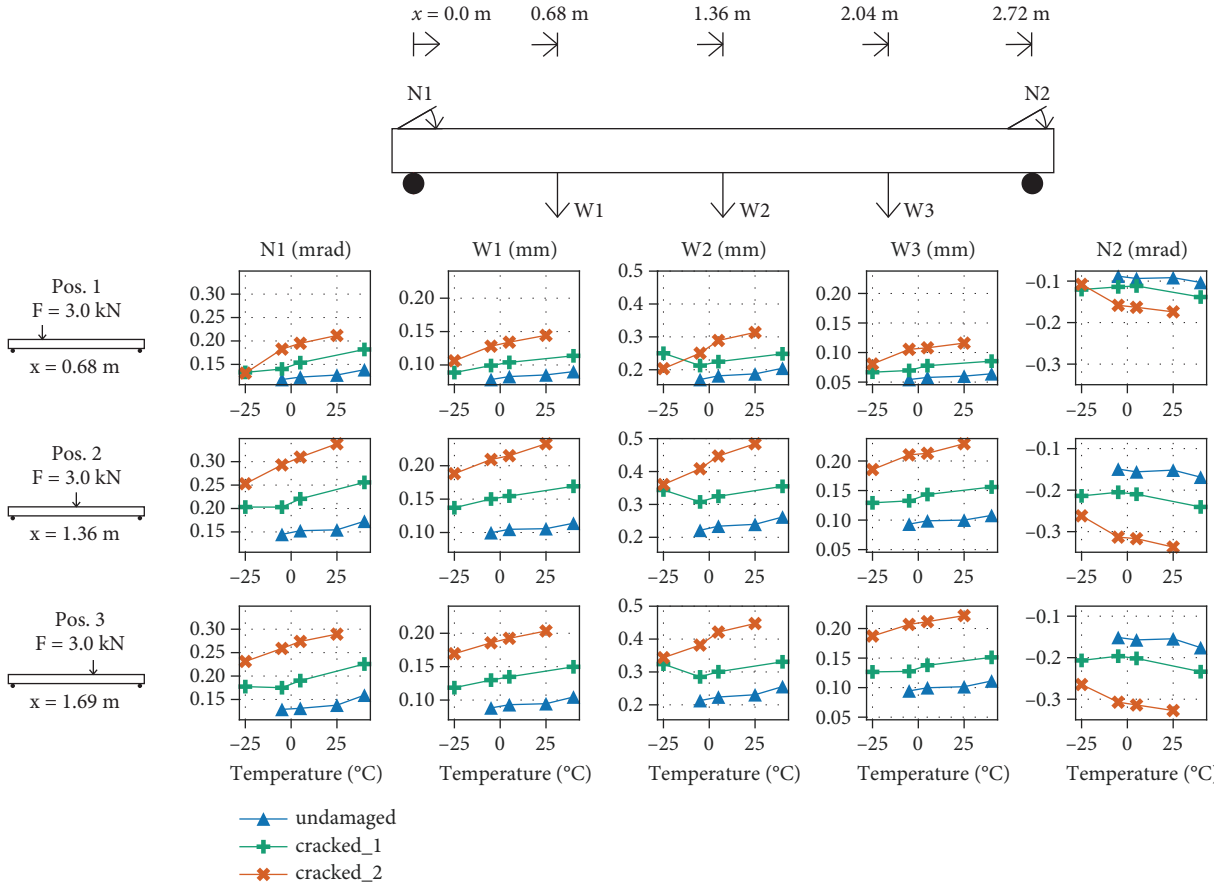

FIGURE 6: Sensor setup (top), load positions (left), and postprocessed data (center). Each subplot consists of observed deflections or inclinations as a function of temperature. Each column corresponds to a sensor (N1, W1, W2, W3, and N2) and each row to a load position.

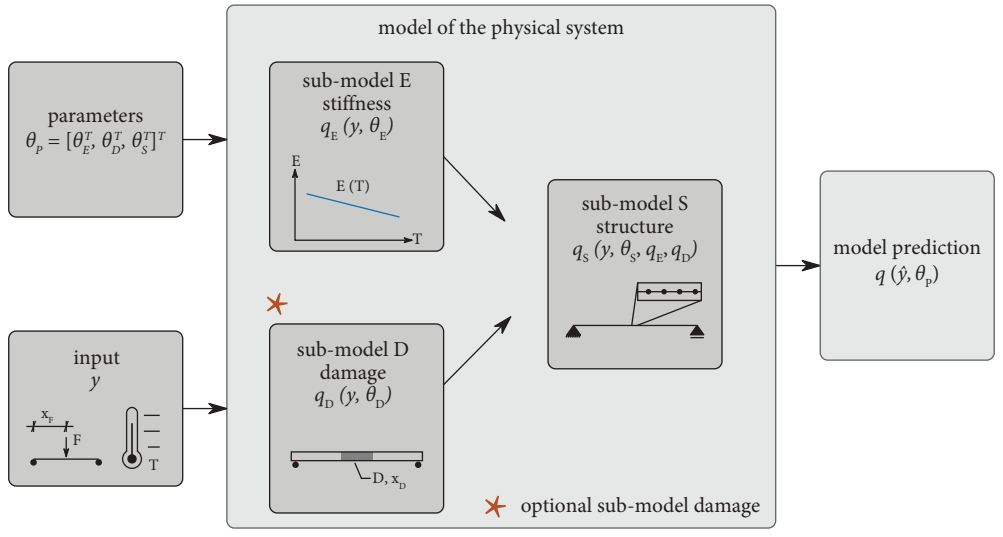

FIGURE 7: Deterministic system model of the RC beam.

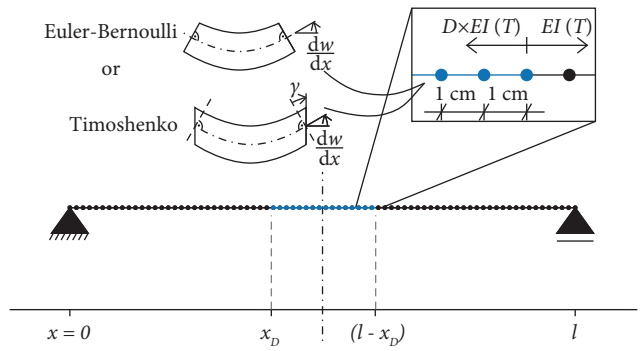

FIGURE 8: FE model of the RC beam together with illustrations of the Euler–Bernoulli and Timoshenko beam theory and the cracked region resulting from the three-point bending test.

jointly represented by uncertain prediction errors $\varepsilon_i = [\varepsilon_{W1,i}, \varepsilon_{W2,i}, \varepsilon_{W3,i}, \varepsilon_{N1,i}, \varepsilon_{N2,i}]^T$ (see also Section 2.3). We assume that the prediction errors ε_i are Gaussian-distributed with mean $b = [b_{W1}, b_{W2}, b_{W3}, b_{N1}, b_{N2}]^T$ and covariance matrix Σ_ε, i.e.,

$$\varepsilon_i \sim \mathcal{N}(\varepsilon_i; b, \Sigma_\varepsilon). \tag{19}$$

The mean b can be interpreted as a bias representing systematic deviations of the model predictions from the observations. The covariance matrix Σ_ε describing the dependence among the different components of ε_i can be constructed as follows:

$$\Sigma_\varepsilon = D \times R \times D, \tag{20}$$

where

$$D = \mathrm{diag}(\sigma_{W1}, \sigma_{W2}, \sigma_{W3}, \sigma_{N1}, \sigma_{N2}), \tag{21}$$

is the diagonal matrix of the standard deviation $\sigma = [\sigma_{W1}, \sigma_{W2}, \sigma_{W3}, \sigma_{N1}, \sigma_{N2}]^T$ of the different components of ε_i and R is the symmetrical correlation matrix. To determine the components of R, we adopt an exponential correlation function [29]:

$$r(x_1, x_2) = \exp\left(-\frac{|x_1 - x_2|}{l_\rho}\right), \tag{22}$$

in which $|x_1 - x_2|$ is the distance between two sensors, and l_ρ is the *correlation length*.

We assume that there is no cross-correlation between prediction errors ε_i and ε_j, which are associated with two separate observations i and j.

The bias b, the standard deviation σ, and the correlation length l_ρ are the uncertain parameters of the prediction error model. These parameters are collected in the parameter vector θ_ε.

3.3.5. Likelihood Function. The likelihood function $L(\theta \mid \mathcal{D}_i)$ describing the relation between the ith dataset $\mathcal{D}_i = \{\hat{z}_i, \hat{y}_i\}$ and the uncertain parameters $\theta = [\theta_p^T, \theta_\varepsilon^T]^T$ is formulated according to Section 2.4. Since the prediction errors ε_i are here modeled with a mean b instead of a zero mean, the measure-of-fit function $J(\theta, D_i)$ defined in equation (4) becomes

$$J(\theta, D_i) = \frac{1}{2}\left[\hat{z}_i - q(\hat{y}_i, \theta_p) - b\right]^T \Sigma_\varepsilon^{-1}(\theta_\varepsilon)\left[\hat{z}_i - q(\hat{y}_i, \theta_p) - b\right]. \tag{23}$$

The joint likelihood function $L(\theta \mid \mathcal{D})$ describing all available data $\mathcal{D}$ is constructed according to equation (5). This modeling approach is applied for each stochastic model class considered in the current case study.

3.3.6. Prior Probabilistic Model of the Model Parameters. Throughout this case study, the uncertain model parameters $\theta = [\theta_p^T, \theta_\varepsilon^T]^T$ of each stochastic model class are a priori modeled as independent random variables. Consequently, their joint prior distribution is simply the product of their prior marginal distributions, which are defined based on the existing literature [19, 34] and engineering judgment (see Table 1). The prior distributions of the damage parameters D and x_D are estimated through an analytical analysis of the properties of the cracked section. A choice of large standard deviations ensures these priors are weakly informative.

Following [19], Young's modulus of concrete is assumed to follow a log-normal distribution with a coefficient of variation (CV) of 0.15. The mean value for the bending stiffness of the uncracked section at 0°C is $\mathrm{EI}_0 = 33.3\,\mathrm{GPa} \times 26667\,\mathrm{cm} = 8.8\,\mathrm{MNm}^2$.

According to the existing literature [34], Poisson's ratio of concrete ν_c varies from the lower bound of 0.14 to the upper bound of 0.26. As a prior distribution for ν_c, we, thus, select a truncated normal distribution within these bounds with a mean of 0.2 and a coefficient of variation of 0.15.

A preliminary analysis of the data shown in Figure 6 reveals that there is a 0.1 mm offset between the observed deflections at the position of the displacement transducer $W2$ and the corresponding deflections predicted by a simple hand calculation. Therefore, a prior distribution of the mean of the prediction error $\varepsilon_{W2,i}$ is chosen to account for this offset.

3.4. Model Building. The first goal of this case study is to identify the most suitable modeling approach for the RC beam based on the data from the reference phase, i.e., the data collected from the *uncracked* beam. To this end, several modeling choices are considered. Each of these modeling choices addresses a context- and problem-specific question. In the current case study, the following four questions arise.

Table 1: Prior marginal distributions of the model parameters $\theta = [\theta_p^T, \theta_\varepsilon^T]^T$ defined in terms of the distribution type, mean, and standard deviation (SD).

Parameter	Distribution	Mean	SD
Bending stiffness at 0°C (EI_0)	Log-normal	8.8 MNm^2	0.15×8.8 MNm^2
Temperature-sensitivity (α)	Normal	−0.01 MNm^2/K	0.25×-0.01 MNm^2/K
Poisson's ratio (ν_c)	Truncated normal[1]	0.2	0.15×0.2
Stiffness reduction due to damage (D)	Beta[2]	0.29	0.16
Extent of cracked region (x_D)	Truncated normal[3]	0.68 m	0.20×0.68 m
SD of pred. error at $W1$ (σ_{W1})	Log-normal	0.01 mm	0.50×0.01 mm
SD of pred. error at $W2$ (σ_{W2})	Log-normal	0.01 mm	0.50×0.01 mm
SD of pred. error at $W3$ (σ_{W3})	Log-normal	0.01 mm	0.50×0.01 mm
SD of pred. error at $N1$ (σ_{N1})	Log-normal	0.015 mrad	0.50×0.015 mrad
SD of pred. error at $N2$ (σ_{N2})	Log-normal	0.015 mrad	0.50×0.015 mrad
Correlation length of errors (l_ρ)	Log-normal	1.4 m	1.00×1.4 m
Mean of pred. error at $W1$ (b_{W1})	Normal	0.0 mm	0.15×0.001 mm
Mean of pred. error at $W2$ (b_{W2})	Normal	0.1 mm	0.50×0.1 mm
Mean of pred. error at $W3$ (b_{W3})	Normal	0.0 mm	0.15×0.001 mm
Mean of pred. error at $N1$ (b_{N1})	Normal	0.0 mrad	0.15×0.0015 mrad
Mean of pred. error at $N2$ (b_{N2})	Normal	0.0 mrad	0.15×0.0015 mrad

[1]Limited to values between 0.14 and 0.26, as indicated in [4]. [2]Defined for values between 0.0 and 1.0, with a mode of 0.2. [3]Limited to values between 0.0 m and 1.36 m.

3.4.1. Should the RC Beam be Modeled According to Euler–Bernoulli or Timoshenko Beam Theory? A fundamental question in modeling structures is whether the applied mechanical theory is appropriate to describe the relevant structural behavior. In the current case, the most prominent question is whether the RC beam can be modeled as an Euler–Bernoulli beam or a Timoshenko beam.

3.4.2. Should Poisson's Ratio be Modeled as a Random Variable? The flexural stiffness EI_0 at 0°C and the temperature-sensitivity of the flexural stiffness α are parameters of the system model describing the temperature-dependent structural behavior of the RC beam. These parameters are modeled as random variables in each stochastic model class. If the beam is modeled according to Timoshenko beam theory, Poisson's ratio ν_c is an additional parameter of the structural system model, which is typically deterministically set to 0.2 for hardened concrete. The question is whether ν_c should be included in the model updating by modeling it as a random variable with a prior distribution that explicitly quantifies the *prior* assumptions about its plausible values.

3.4.3. Are All Bias Terms Required? Modeling the prediction errors ε_i with a nonzero mean—as discussed in Section 3.3.4—introduces additional and possibly unnecessary model parameters. This approach could lead to overfitting, and it is thus reasonable to compare stochastic model classes *with* and *without* these biases. It seems plausible to include at least the bias of the prediction error associated with the deflection $W2$ at the mid-span of the beam. However, the biases of the prediction errors corresponding to the remaining four observable quantities (i.e., the rotations at the bearings and the deflections at the quarter-span of the beam) may not be required.

3.4.4. Is a Submodel for the Temperature-Dependent Material Behavior Required? The broader question of overfitting concerns the inclusion of a submodel of the environmental and operational variability (EOV). In this case study, the question is whether the model of the temperature-dependent flexural stiffness of the RC beam is required.

3.4.5. Model Class Selection. Among the set of possible stochastic model classes, the most suitable one is found with the help of model quality indicators defined in Section 2.5. While the evidence c_E and the model class selection factor MSF are considered the most appropriate indicators in the Bayesian context, the AIC* and BIC* are also evaluated.

A total number of 2^n stochastic model classes can be formulated if n "binary" modeling choices (with two alternatives each) are available. Even for a small number of such modeling choices, an exhaustive comparison of all possible stochastic model classes is unfeasible. For this reason, it is necessary to reduce the number of stochastic model classes considered in the model building. To this end, an iterative strategy is applied, in which—starting from the most complex stochastic model class—two stochastic model classes are defined for a given modeling choice and compared. The one indicating a higher model quality is subsequently used as a starting point for identifying the next best modeling choice, and so on. This approach led to a total of 5 combinations of modeling choices considered in the current case study, which are summarized in Table 2. The most plausible stochastic model class is, henceforth, referred to as *base model class*.

Table 2: Overview of the modeling choices associated with each considered stochastic model class.

Stochastic model class	Beam theory	ν_c	Biases	SM EOV
Base model class	Timoshenko	0.2	All	✓
Euler–Bernoulli	Euler–Bernoulli	0.2	All	✓
Probabilistic ν_c	Timoshenko	Random var.	All	✓
Only one bias	Timoshenko	0.2	Only W2	✓
Excl. EOV	Timoshenko	0.2	All	×

In Table 3, the model quality indicators introduced in Section 2.5 for all stochastic model classes are provided. It confirms that the base model class is the *most plausible* class, conditional on the data from the reference phase.

3.5. Uncertainty Quantification. The various uncertainties described in Section 2.3—the model and observation uncertainties (which are here jointly represented by a prediction error model), parameter uncertainties, and the resulting prediction uncertainties—are quantified for the base model class conditional on the load test data from the uncracked beam.

In the following, the information gain resulting from the model updating is measured in terms of the Kullback–Leibler divergence [39] of the posterior from the prior distribution and expressed in *Shannon (Sh)*—also known as *bit*. Note that an information gain of one Sh reduces the uncertainty by a factor of 2.

The prior and posterior marginal distributions of the parameters with *physical* meaning—i.e., EI_0 and α—are shown in Figure 9. They quantify the initial and updated *parameter uncertainties*. A significant amount of information is gained on EI_0 (1.5 Sh). In this case, the CV reduces from 0.15 to 0.01. Only a moderate amount of information is gained on the parameter α (0.3 Sh).

The prior and posterior marginal distributions of the mean of the prediction errors associated with each observed quantity are shown in Figure 10. 2.7 Sh and 1.2 Sh of information are gained on the biases b_{W1} and b_{W2} of the prediction errors corresponding to displacements $W1$ and $W2$. 0.93 Sh of information are gained on the bias b_{N1} of the prediction errors associated with rotation $N1$. Notably, the prior estimate of the offset of the displacement transducer $W2$ at the mid-span of the beam is confirmed to be plausible and updated from centering around 0.1 mm to centering around 0.09 mm.

The prior and posterior marginal distributions of the parameters representing the standard deviation and correlation of the prediction errors associated with each observed quantity are shown in Figure 11. In this case, the uncertainties are reduced by a moderate amount, i.e., the CV of these parameters reduces from 0.5 to values ranging between 0.37 and 0.19. Most information is gained on the standard deviation of the prediction errors corresponding to the displacement $W1$ (1.1 Sh). Note that the posterior CV of σ_{W1} and σ_{W2} are similar (0.19), but the information gain is different (1.1 Sh vs. 0.58 Sh) because the posterior marginal distribution of σ_{W1} differs more from the corresponding prior marginal distribution compared to σ_{W2}.

Table 3: Model class selection with model quality indicators of all considered stochastic model classes.

Probabilistic model class	AIC*	BIC*	$\ln c_E$	MSF
Base model class	220.1	216.9	206.0	0.515
Euler–Bernoulli	218.5	215.3	205.3	0.274
Probabilistic ν_c	219.9	216.5	205.1	0.212
Only one bias	178.0	175.8	164.2	3.5×10^{-19}
Excluding EOV	205.2	202.3	196.9	2.4×10^{-5}

The model quality indicators are determined based on the data obtained during the diagnostic load tests of the uncracked beam. AIC*, BIC*, c_E, and MSF are calculated according to equations (8), (10), (11), and (14).

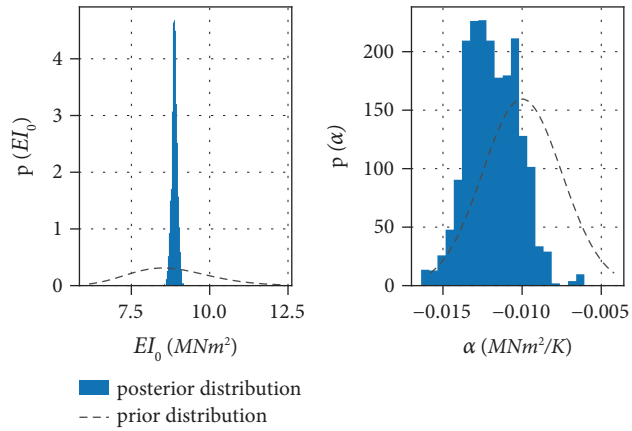

Figure 9: Prior and (empirical) posterior marginal distributions of the *physical* parameters EI_0 and α considered in the base model class. The posterior marginal distributions are conditional on the data from the uncracked beam.

For each considered beam temperature and load position, 3000 samples from the prior and posterior distribution of the model parameters are propagated through the data prediction model considered in the base model class. These evaluations result in probabilistic predictions of the observable quantities, i.e., the observable displacements and rotations. In Figure 12, the prior and posterior mean and the 90% highest density interval (HDI [51]) of the predictions of the observable quantities together with the actual observed data. In addition, the prior and posterior CV is estimated for each predicted observable quantity conditional on the beam temperature and load position. The average of all CVs reduces from 0.1 to 0.032 due to the model updating.

3.6. Damage Identification. In Section 3.4, the proposed Bayesian probabilistic framework was implemented to identify a suitable stochastic model class of the temperature-dependent behavior of the RC beam based on the data from

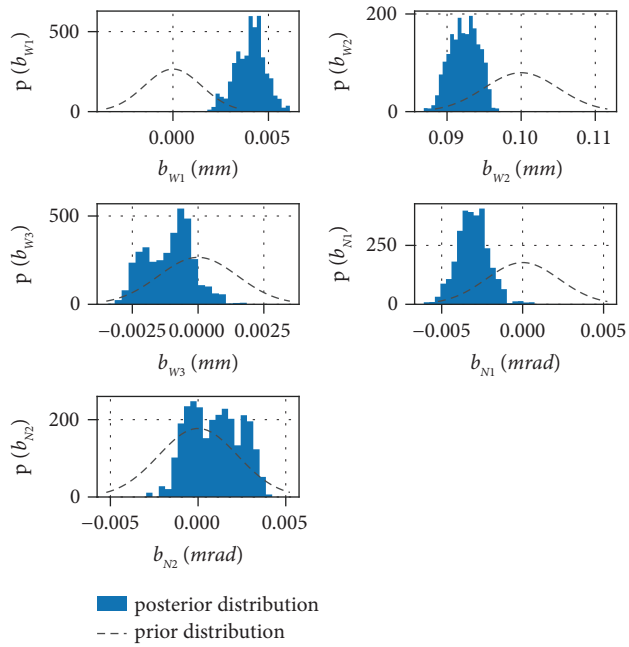

FIGURE 10: Prior and (empirical) posterior marginal distributions of the means of the prediction errors considered in the base model class. The posterior marginal distributions are conditional on the data from the uncracked beam.

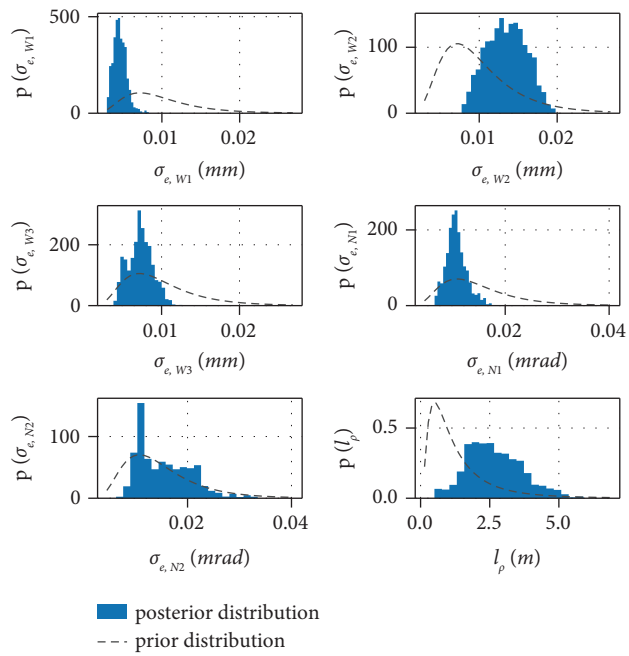

FIGURE 11: Prior and (empirical) posterior marginal distributions of the parameters representing the standard deviation and correlation of the prediction errors considered in the base model class. The posterior marginal distributions are conditional on the data from the uncracked beam.

the *uncracked* RC beam or *reference phase*. The most plausible modeling approach—the base model class—is now chosen as a basis for identifying damage in the *monitoring phase*.

To this end, an additional FE model is first constructed by extending the FE model contained in the base model class with the parameterized submodel describing damage (see Section 3.3.3). Subsequently, two competing stochastic model classes are formulated based on the base model class, in which—as illustrated in Figure 13— the beam is assumed to be undamaged in the reference phase and, depending on the model class, either undamaged or damaged in the monitoring phase.

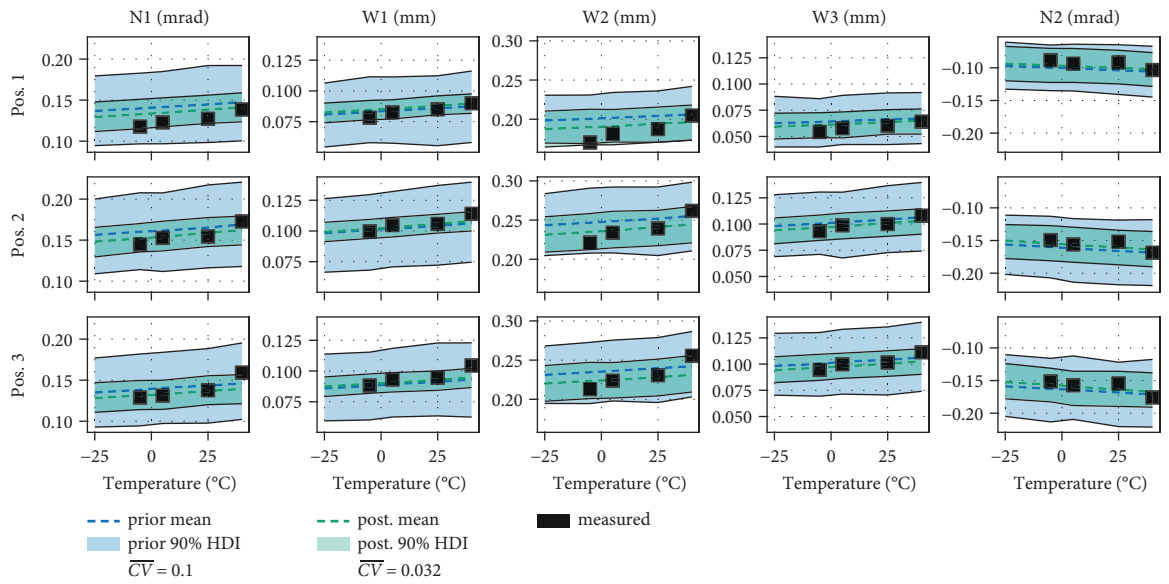

FIGURE 12: Prior and (empirical) posterior mean and the 90% highest density interval of the deflections and inclinations predicted based on the base model class. Each column corresponds to an observable quantity, and each row corresponds to a load position. Each subplot also contains the observed data.

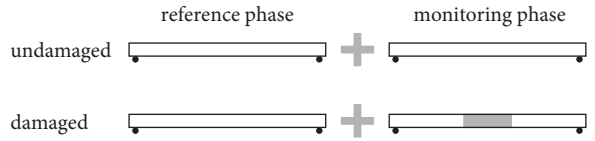

FIGURE 13: Illustration of the two competing stochastic model classes formulated for damage identification in the monitoring phase. Both classes are formulated based on the most plausible stochastic model class identified in the reference phase (see Section 3.4).

In both stochastic model classes, the FE model of the undamaged beam is applied to relate the data from the reference phase to the model parameters. The same FE model is also utilized to relate the data from the monitoring phase to the model parameters in the stochastic model class representing the undamaged beam. In contrast, the FE model of the damaged beam is used to link the data from the monitoring phase with the model parameters in the stochastic model class representing the damaged beam. Within both stochastic model classes, the data from the reference and monitoring phase are sequentially applied to update the probabilistic distributions of the model parameters using the Bayesian analysis. Based on this analysis, damage detection and characterization are performed as discussed in Section 2.6.

3.6.1. Damage Detection. Table 4 summarizes the model quality indicators for both stochastic model classes representing the undamaged and damaged state in the monitoring phase. The indicators are estimated by applying (a) the data from the *uncracked* beam in the reference phase and (b) the data from the beam in either the *uncracked*, *cracked_1*, or *cracked_2* state in the monitoring phase.

The results show that the damaged model class is significantly more plausible if the beam is damaged in the monitoring phase, i.e., data from the damaged RC beam are applied in this phase. The opposite is the case if the beam is undamaged in the monitoring phase.

In addition to the MSF, the Bayes factor (BF) is also computed as described in Section 2.6:

$$\mathrm{BF}_{\mathrm{uncracked}} = \frac{\mathrm{MSF}_{\mathrm{damaged|uncracked}}}{\mathrm{MSF}_{\mathrm{undamaged|uncracked}}} = \frac{2.0 \times 10^{-5}}{1 - \left(2.0 \times 10^{-5}\right)} \approx 2.0 \times 10^{-5}, \tag{24}$$

$$\mathrm{BF}_{\mathrm{cracked\_1}} = \frac{\mathrm{MSF}_{\mathrm{damaged|cracked\_1}}}{\mathrm{MSF}_{\mathrm{undamaged|cracked\_1}}} = \frac{1 - \left(3.0 \times 10^{-46}\right)}{3.0 \times 10^{-46}} \approx 3.3 \times 10^{45}, \tag{25}$$

Table 4: Model class selection considering the stochastic model classes representing the undamaged and damaged in the monitoring phase. The analysis considers data from the undamaged RC beam in the reference state and data obtained from all different states of the beam in the monitoring phase.

Data applied in the monitoring phase	Stochastic model class	AIC*	BIC*	$\ln c_E$	MSF
Uncracked	Undamaged	460.4	457.3	437.5	$1.0-(2.0\times10^{-5})$
	Damaged	455.6	451.9	426.6	2.0×10^{-5}
cracked_1	Undamaged	274.3	271.2	261.5	3.0×10^{-46}
	Damaged	376.9	373.2	366.4	$1.0-(3.0\times10^{-46})$
cracked_2	Undamaged	185.2	182.0	149.1	1.4×10^{-71}
	Damaged	321.6	318.0	312.3	$1.0-(1.4\times10^{-71})$

AIC*, BIC*, c_E, and MSF are calculated according to equations (8), (10), (11), and (14).

$$\mathrm{BF}_{\mathrm{cracked\_2}}=\frac{\mathrm{MSF}_{\mathrm{damaged|cracked\_2}}}{\mathrm{MSF}_{\mathrm{undamaged|cracked\_2}}}=\frac{1-\left(1.4\times10^{-71}\right)}{1.4\times10^{-71}}\approx7.1\times10^{70}. \tag{26}$$

$\mathrm{BF}_{\mathrm{cracked\_1}}$ and $\mathrm{BF}_{\mathrm{cracked\_2}}$ provide a strong indication of damage when the RC beam is in the *cracked_1* or *cracked_2* state in the monitoring phase. $\mathrm{BF}_{\mathrm{uncracked}}$ confirms that the beam is undamaged when it is in the *uncracked* state in the monitoring phase.

3.6.2. Damage Characterization. With the proposed method, the *location* and *severity* of the damage in the beam can be characterized based on the posterior marginal distributions of the model parameters x_D and D. As an illustration, consider the case in which data obtained from the RC beam in the *cracked_2* state are applied in the monitoring phase. For this case, the prior and posterior marginal distributions of x_D and D are shown in Figure 14 together with the prior and posterior marginal distributions of EI_0 and α.

The cracked region of the RC beam has an average flexural stiffness of $9.1\,\mathrm{MNm}^2\times0.32=2.9\,\mathrm{MNm}^2$ and is predicted to start approximately 1.0 m away from both supports. The predicted extent of the cracked region is consistent with the cracks observed after the three-point-bending test. Conditional on the considered data, the parameters D and x_F are highly correlated with a correlation factor $\rho=-0.91$ as confirmed by their posterior distribution shown in Figure 15.

4. Numerical Validation

The case study described in the previous section demonstrates the capabilities of the proposed framework for model building and damage identification. However, the question remains how valid the results are since the *true* values of the model parameters $\theta=[\theta_p^T,\theta_\varepsilon^T]^T$ are unknown. To validate the proposed approach, a numerical study is performed. First, synthetic data of the observable deformation response of the undamaged and damaged RC beam are generated using fixed values of the parameters $\theta=[\theta_p^T,\theta_\varepsilon^T]^T$ as described in Section 4.1. These parameter values represent the *true* parameter values in this numerical study. Subsequently, the workflow for damage identification is implemented based on the synthetic data as described in Section 4.2. In this way, we seek to determine how well the updated probabilistic distributions of the model parameters agree with the *true* parameter values.

4.1. Synthetic Data. Synthetic data of the observable structural response are generated for five beam temperatures in (a) the reference and (b) the monitoring phase, based on the data prediction model (see also equation (2)) contained in the *base model class*. In this process, the FE model of the undamaged RC beam with parameters EI_0 and α and the FE model of the damaged RC beam parameters EI_0, α, D, and x_D are, respectively, embedded in the data prediction model. The applied values of the parameters of the FE models and probabilistic error model are compared to the posterior marginal distributions of the parameters in Section 4.3.

4.2. Damage Identification

4.2.1. Damage Detection. To demonstrate the damage detection capability, two competing stochastic model classes are defined in the same way as described in Section 3.6 and illustrated in Figure 13. Subsequently, the synthetic data generated based on the undamaged beam model are applied in the reference phase and the data generated based on the damaged beam model are utilized in the monitoring phase. The model quality indicators computed based on the synthetic data are listed in Table 5. They clearly indicate that the damaged model class is more plausible. The Bayes factor of $\mathrm{BF}\approx1.9\times10^{36}$ also supports this assessment.

4.2.2. Damage Characterization. After selecting the most likely model class, the posterior marginal distributions of the corresponding model parameters are compared with the *true* parameter values used for data simulation. The posterior marginal distributions of the parameters of the physical models are shown in Figure 16. There appears to be a good agreement between the respective posterior mean values and the known *true* values. More importantly, all posterior marginal distributions contain the *true* values of the physical parameters.

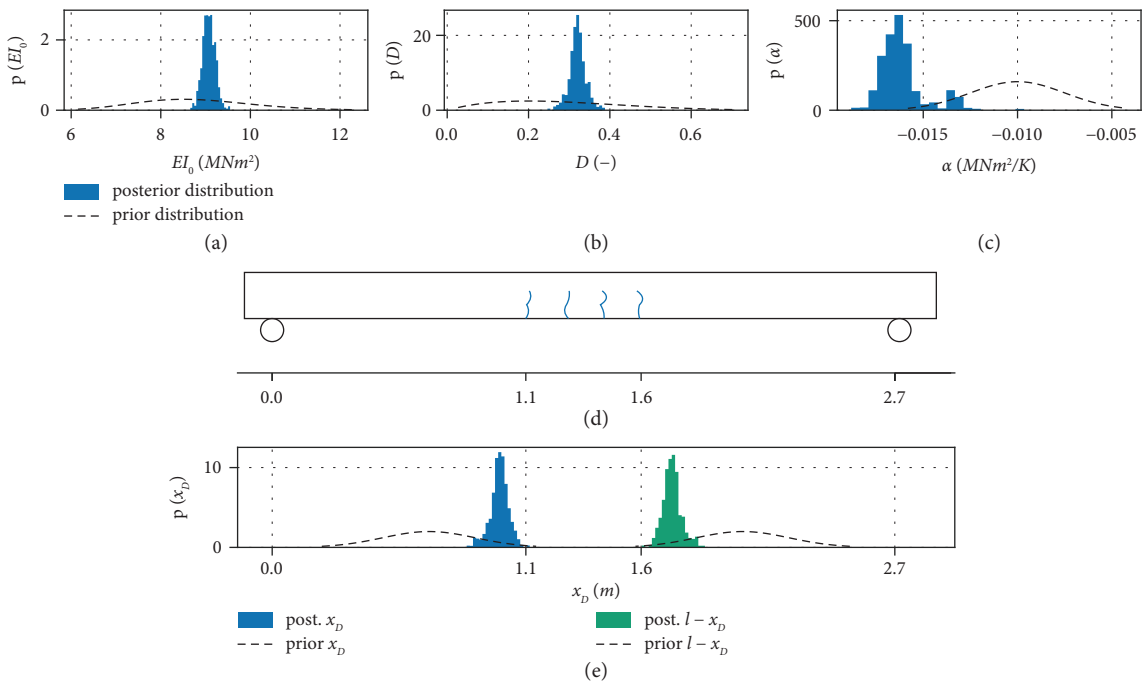

FIGURE 14: Prior and (empirical) posterior marginal distributions of the *physical* parameters of the base model class with additional submodel for damage: (a) bending stiffness EI_0 at 0°C, (b) stiffness reduction D, (c) temperature-sensitivity α, and (e) symmetrical start and end of the extent of the cracked region quantified in terms of x_D. Subfigure (d) indicates the extent of the cracks observed after the three-point bending test with a maximum load of 28 kN. This corresponds to the *cracked_2* state of the beam.

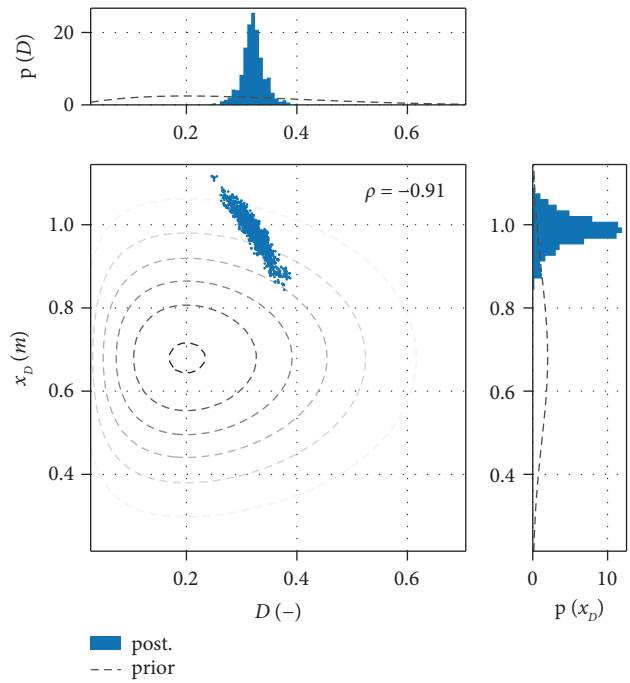

FIGURE 15: Joint and marginal prior and (empirical) posterior distribution of the *damage-related* parameters of the base model class. The posterior distributions are conditional on the data obtained in the monitoring phase from the beam in the *cracked_2* state.

Table 5: Model class selection of the damaged and undamaged stochastic model classes based on the synthetic data.

Stochastic model class	AIC*	BIC*	$\ln c_E$	MSF
Undamaged	388.2	383.6	377.7	5.4×10^{-37}
Damaged	469.1	463.8	461.2	$1.0-(5.4\times10^{-37})$

AIC*, BIC*, c_E, and MSF are calculated according to equations (8), (10), (11), and (14).

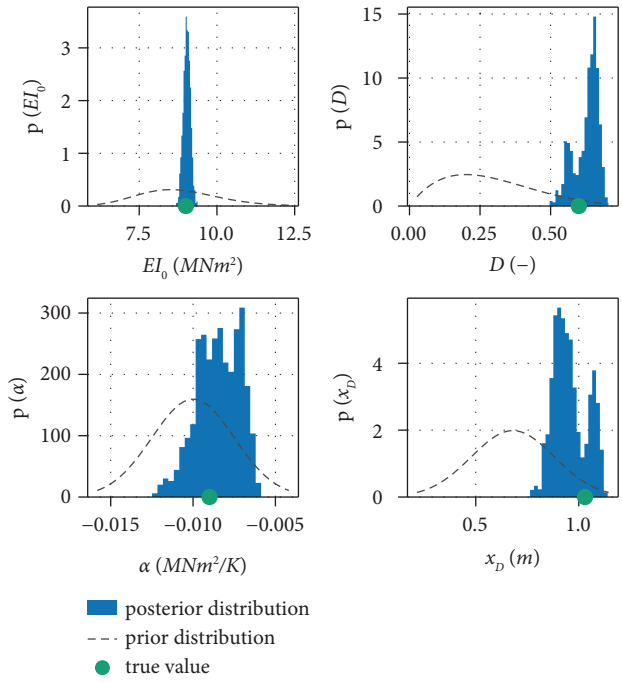

Figure 16: Prior and (empirical) posterior marginal distributions of the *physical* parameters of the damaged model class together with the *true* parameter values.

4.3. Results of All Parameters. To assess the quality of the updated distributions of all model parameters, their *true* parameter values are compared with the 90% highest density interval (HDI [51]) of the corresponding posterior marginal distributions in Table 6.

The *true* values of all and one parameter (b_{W1}) lie within the corresponding the 90% HDI of the posterior distribution. These results indicate that the results of the case study presented in Section 3 are credible.

5. Discussion

To address the need for damage detection and especially characterization in structural health monitoring under environmental and operational variability, we introduce a model-building framework for damage identification. It enables the inclusion of effects of environmental and operational conditions based on physical principles. The formal model-building procedure addresses the problems of choosing the most appropriate model sophistication as well as parametrization by leveraging indicators of model quality. These indicators are also used for the detection of damage by comparing probabilistic model classes with and without submodels for damage. These submodels for damage are parameterized, thus enabling further characterization of damage.

The proposed framework was applied in an experimental case study. The challenges of working with real data (which were even corrupted by a faulty sensor) and finding the most appropriate model sophistication and parametrization could be addressed. The characterization of the damage in terms of size and location was congruent with the observed cracks in the concrete beam. However, the damage introduced in the specimen was relatively large. In practice, it has to be ensured that the potential structural damage defined in terms of type, location, and severity can be identified from the monitoring data. Thus, the design of an SHM system and the type of monitoring data are governed by the potential structural damages that need to be identified.

The damage characterization relies on the identification of parameters, which in laboratory or real-world structures cannot be known with certainty. Therefore, a numerical study was conducted to validate the parameter identification. All known *true* parameters lay within the 90% highest density interval of the posterior distributions of the parameters. This can be interpreted as a confirmation of the damage characterization capability.

To search the space of modeling choices for the most appropriate probabilistic model class, a heuristic method was proposed, iteratively comparing two model classes for each choice, and taking the more probable model class as the basis for the assessment of the next modeling choice.

Table 6: Comparison of *true* parameter values with the 90% highest density interval (HDI) of their posterior distributions.

Parameter	True value	Post mean	90% HDI
Bending stiffness at 0°C (EI_0)	9.00 MNm^2	9.03 MNm^2	(8.83; 9.19) MNm^2
Temperature-sensitivity (α)	−0.009 MNm^2/K	−0.00847 MNm^2/K	(−0.0104; −0.00645) MNm^2/K
Stiffness reduction due to damage (D)	0.6	0.627	(0.555; 0.683)
Extent of cracked region (x_D)	1.03 m	0.956 m	(0.86; 1.11) m
SD of pred. error at $W1$ (σ_{W1})	0.009 mm	0.0105 mm	(0.00819; 0.013) mm
SD of pred. error at $W2$ (σ_{W2})	0.008 mm	0.00837 mm	(0.0069; 0.00977) mm
SD of pred. error at $W3$ (σ_{W3})	0.012 mm	0.0117 mm	(0.00903; 0.0139) mm
SD of pred. error at $N1$ (σ_{N1})	0.013 mrad	0.0123 mrad	(0.0095; 0.0148) mrad
SD of pred. error at $N2$ (σ_{N2})	0.016 mrad	0.015 mrad	(0.0125; 0.0174) mrad
Correlation length of errors (l_ρ)	0.9 m	1.1 m	(0.0765; 1.4) m
Mean of pred. error at $W1$ (b_{W1})	0.003 mm	0.00128 mm	$(-5.54\times10^{-5}$; 0.00256) mm
Mean of pred. error at $W2$ (b_{W2})	0.112 mm	0.110 mm	(0.107; 0.112) mm
Mean of pred. error at $W3$ (b_{W3})	−0.002 mm	−0.0017 mm	(−0.00297; −0.000782) mm
Mean of pred. error at $N1$ (b_{N1})	−0.001 mrad	−0.000414 mrad	(−0.00179; 0.00201) mrad
Mean of pred. error at $N2$ (b_{N2})	0.002 mrad	0.00109 mrad	(−0.000913; 0.0033) mrad

There is no proof that this strategy guarantees finding the most appropriate probabilistic model class. Other strategies are possible—an example of a strategy for hierarchical model class selection for damage represented by substructuring is introduced in [52]. This shortcoming can be alleviated by searching the whole space of modeling choices.

In this contribution, we merged model uncertainty and observation uncertainty in the prediction error. This impedes the full separation of sources of uncertainty. However, interpreting the contribution of different sources of uncertainty is still possible to some extent by examining the parameters for the mean and standard deviation of the prediction errors of the individual measured quantities.

6. Concluding Remarks

This contribution introduces a formal procedure for the inclusion of model updating in damage identification. This procedure constitutes an approach to build structural models for structural health monitoring considering environmental variability. The novelty of this procedure is twofold: First, structural models are extended by submodels to explicitly capture the effect of environmental variability and potential structural damages. Second, a methodological workflow is proposed to identify the most suitable model to represent a structural system subject to environmental variability and to identify damage in this structural system. The intended use case is to apply observed data in conjunction with models and prior engineering knowledge for the characterization of damage. This is a steppingstone for the performance assessment of monitored structures and a path to optimizing inspection and maintenance. Quantifying uncertainties in the damage state of structural systems is paramount for a reliability-based and code-based performance assessment. The approach can be extended to capture time-dependent deterioration processes.

The case study shows the potential of this approach, but the assessed limitations highlight areas where further research is needed:

(i) Real-world structures–benchmark: The case study presented in this contribution rests on laboratory experiments and simulations with synthetic monitoring data. As with all SHM frameworks, a case study considering a real-world structure would be desirable, ideally with damage occurring during the monitoring phase [8, 11, 14, 29].

(ii) Real-world structures–algorithmic improvements: For real-world structures, which can be orders of magnitude larger than the specimen in this case study, performance is an issue in sampling-based Bayesian model updating since the evaluation of the likelihood function for a given sample usually requires the solution of a large finite-element model. The parallelization of sampling algorithms [53] or the use of surrogate models [14] are possible solutions.

(iii) Smaller damages and more complex temperature-dependent structural behavior: This case study considered a relatively simple structural system with a relatively simple temperature-dependent structural behavior and relatively large structural damage. The next step in the performance assessment of the proposed framework should consider more complex temperature-dependent structural behavior in combination with smaller damages. Ideally, it would be applied in a real-world scenario [42].

(iv) Optimization of data collection: The probabilistic model-building framework introduced in Section 2 includes the (optional) optimization of the data-collecting process considering the postulated probabilistic model classes and the data from the reference phase. For example, the sensor placement can be optimized, or measurement campaigns can be planned accordingly. The procedures and applied methods for this step need to be developed and investigated [25].

(v) Modeling choices concerning model and observation uncertainties: The choices of modeling the model and observation uncertainties influence the

inference [28] and thus the posterior prediction uncertainty. More work is needed to catalog the possible modeling approaches and investigate them. First research concerning different temporal and spatial correlations has already been conducted [29]. Hierarchical modeling of structural parameters [15, 42] could also be considered.

(vi) Improved model class selection: In our contribution, model class selection is purely based on the observed data and the model classes themselves. Considering other factors such as maintenance decisions based on forecasted data and predictions from updated model classes or the computational expense of evaluating the models [54] could improve the model selection. However, adopting such strategies may require the use of alternative approaches, such as decision-theoretic methods [54].

(vii) Further effects of environmental and operational variability: Temperature effects are a major influence on the environmental variability in structural systems [6, 10]. However, there are additional influences that may have to be considered, such as variable support conditions, and varying mass, wind, and traffic loads [8, 9, 11]. Further studies can include submodels of these effects. This also includes heteroscedasticity of the measured data induced by environmental effects, e.g., due to variable typhoon conditions [11].

Data Availability

The data used to support the findings of this study are available from the corresponding author upon request.

Conflicts of Interest

The authors declare that there are no conflicts of interest regarding the publication of this article.

Authors' Contributions

Patrick Simon conceptualized the study, was involved in data curation, performed formal analysis, investigated the data, developed methodology, was responsible for software, visualized the study, and wrote the original draft. Ronald Schneider was responsible for funding acquisition, conceptualized the study, investigated the data, developed methodology, was involved in project administration, supervised the study, validated the data, and reviewed and edited the manuscript. Matthias Baeßler was responsible for funding acquisition and resources, supervised the study, and reviewed and edited the manuscript. Guido Morgenthal was responsible for funding acquisition, supervised the study, and reviewed and edited the manuscript.

Acknowledgments

The support of the colleagues at BAM during the execution of the experiment is gratefully acknowledged. This work was supported by the German Federal Ministry of Education and Research (BMBF) through grant 13N14658 and VDI Technologiezentrum (VDI TZ). Open access funding was enabled and organized by Projekt DEAL.

References

[1] C. Ye, S.-C. Kuok, L. J. Butler, and C. R. Middleton, "Implementing bridge model updating for operation and maintenance purposes: examination based on UK practitioners' views," *Structure and Infrastructure Engineering*, vol. 18, no. 12, pp. 1638–1657, 2022.

[2] Highways England, "Assessment of highway bridges and structures," 2022, https://www.standardsforhighways.co.uk/dmrb/.

[3] Bundesministerium für Verkehr, "Bau und Stadtentwicklung, Richtlinie zur Nachrechnung von Straßenbrücken im Bestand (Nachrechnungsrichtlinie), Bundesministerium für Verkehr," Bau und Stadtentwicklung, Berlin, Germany, 2011.

[4] M. Baeßler and F. Hille, "A study on diverse strategies for discriminating environmental from damage based variations in monitoring data," in *Proceedings of the Ninth International Conference on Bridge Maintenance, Safety and Management (IABMAS 2018)*, Melbourne, Australia, July 2018.

[5] C. R. Farrar and N. A. J. Lieven, "Damage prognosis: the future of structural health monitoring," *Philosophical Transactions of the Royal Society A: Mathematical, Physical and Engineering Sciences*, vol. 365, no. 1851, pp. 623–632, 2007.

[6] Q. Han, Q. Ma, J. Xu, and M. Liu, "Structural health monitoring research under varying temperature condition: a review," *Journal of Civil Structural Health Monitoring*, vol. 11, no. 1, pp. 149–173, 2020.

[7] H. Sohn and K. H. Law, "A Bayesian probabilistic approach for structure damage detection," *Earthquake Engineering and Structural Dynamics*, vol. 26, no. 12, pp. 1259–1281, 1997.

[8] F. Magalhães, Á. Cunha, and E. Caetano, "Vibration based structural health monitoring of an arch bridge: from automated OMA to damage detection," *Mechanical Systems and Signal Processing*, vol. 28, pp. 212–228, 2012.

[9] H. Sohn, "Effects of environmental and operational variability on structural health monitoring," *Philosophical Transactions of the Royal Society A: Mathematical, Physical and Engineering Sciences*, vol. 365, no. 1851, pp. 539–560, 2007.

[10] Y. Xia, B. Chen, S. Weng, Y.-Q. Ni, and Y.-L. Xu, "Temperature effect on vibration properties of civil structures: a literature review and case studies," *Journal of Civil Structural Health Monitoring*, vol. 2, no. 1, pp. 29–46, 2012.

[11] Q.-A. Wang, Q. Liu, Z. G. Ma et al., "Data interpretation and forecasting of SHM heteroscedastic measurements under typhoon conditions enabled by an enhanced Hierarchical sparse Bayesian Learning model with high robustness," *Measurement*, vol. 230, 2024.

[12] Q.-A. Wang, C. Zhang, Z.-G. Ma, and Y.-Q. Ni, "Modelling and forecasting of SHM strain measurement for a large-scale suspension bridge during typhoon events using variational heteroscedastic Gaussian process," *Engineering Structures*, vol. 251, 2022.

[13] A. Kamariotis, E. Chatzi, and D. Straub, "A framework for quantifying the value of vibration-based structural health monitoring," *Mechanical Systems and Signal Processing*, vol. 184, 2023.

[14] Q. Xia, Y. Xia, H.-P. Wan, J. Zhang, and W.-X. Ren, "Condition analysis of expansion joints of a long-span suspension bridge through metamodel-based model updating considering thermal effect," *Structural Control and Health Monitoring*, vol. 27, no. 5, p. e2521, 2020.

[15] I. Behmanesh and B. Moaveni, "Accounting for environmental variability, modeling errors, and parameter estimation uncertainties in structural identification," *Journal of Sound and Vibration*, vol. 374, pp. 92–110, 2016.
[16] J. L. Beck, "Bayesian system identification based on probability logic," *Structural Control and Health Monitoring*, vol. 17, no. 7, pp. 825–847, 2010.
[17] R. Schneider, S. Thöns, and D. Straub, "Reliability analysis and updating of deteriorating systems with subset simulation," *Structural Safety*, vol. 64, pp. 20–36, 2017.
[18] D. Straub, R. Schneider, E. Bismut, and H.-J. Kim, "Reliability analysis of deteriorating structural systems," *Structural Safety*, vol. 82, 2020.
[19] Joint Comittee on Structural Safety (JCSS), *Probabilistic Model Code*, JCSS, Bengaluru, India, 2001.
[20] P. Simon, R. Schneider, M. Baeßler, and C. Recknagel, "Enhancing structural models with material tests and static response data- a case study considering a steel beam with asphalt layer subject to temperature variations," in *Proceedings of the International Conference on Structural Health Monitoring of Intelligent Infrastructure (SHMII-10)*, Porto, Portugal, July 2021.
[21] E. Ntotsios, C. Papadimitriou, P. Panetsos, G. Karaiskos, K. Perros, and P. C. Perdikaris, "Bridge health monitoring system based on vibration measurements," *Bulletin of Earthquake Engineering*, vol. 7, no. 2, pp. 469–483, 2009.
[22] J. L. Beck and K.-V. Yuen, "Model selection using response measurements: Bayesian probabilistic approach," *Journal of Engineering Mechanics*, vol. 130, no. 2, pp. 192–203, 2004.
[23] K. Worden, C. R. Farrar, G. Manson, and G. Park, "The fundamental axioms of structural health monitoring," *Proceedings of the Royal Society A: Mathematical, Physical and Engineering Sciences*, vol. 463, no. 2082, pp. 1639–1664, 2007.
[24] C. Argyris, S. Chowdhury, V. Zabel, and C. Papadimitriou, "Bayesian optimal sensor placement for crack identification in structures using strain measurements," *Structural Control and Health Monitoring*, vol. 25, no. 5, p. e2137, 2018.
[25] L. Eichner, R. Schneider, and M. Baeßler, "Optimal vibration sensor placement for jacket support structures of offshore wind turbines based on value of information analysis," *Ocean Engineering*, vol. 288, no. 2, 2023.
[26] P. Simon, R. Schneider, E. Viefhues, S. Said, R. Herrmann, and M. Baeßler, "Vibration-based structural health monitoring of a reinforced concrete beam subject to varying ambient temperatures using bayesian methods," in *Proceedings of the EURODYN 2020, XI International Conference on Structural Dynamics*, Athens, Greece, July 2020.
[27] M. C. Kennedy and A. O'Hagan, "Bayesian calibration of computer models," *Journal of the Royal Statistical Society-Series B: Statistical Methodology*, vol. 63, no. 3, pp. 425–464, 2001.
[28] E. Simoen, C. Papadimitriou, and G. Lombaert, "On prediction error correlation in Bayesian model updating," *Journal of Sound and Vibration*, vol. 332, no. 18, pp. 4136–4152, 2013.
[29] I. Koune, Á. Rózsás, A. Slobbe, and A. Cicirello, "Bayesian system identification for structures considering spatial and temporal correlation," *Data-Centric Engineering*, vol. 4, no. 22, p. e22, 2023.
[30] S.-K. Au and F.-L. Zhang, "Fundamental two-stage formulation for Bayesian system identification, Part I: general theory," *Mechanical Systems and Signal Processing*, vol. 66-67, pp. 31–42, 2016.
[31] W. Betz, "Bayesian inference of engineering models," Technische Universität München, München, 2017, Ph.D. thesis.
[32] S. G. S. Pai and I. F. C. Smith, "Methodology maps for model-based sensor-data interpretation to support civil-infrastructure management," *Frontiers in Built Environment*, vol. 8, 2022.
[33] L. S. Katafygiotis and J. L. Beck, "Updating models and their uncertainties. II: model identifiability," *Journal of Engineering Mechanics*, vol. 124, no. 4, pp. 463–467, 1998.
[34] Fédération Internationale du Béton (fib), *Model Code for Concrete Structures 2010*, Ernst and Sohn a Wiley brand, Lausanne, Switzerland, 2013.
[35] A. Bigaj-van Vliet and T. Vrouwenvelder, "Reliability in the performance-based concept of fib Model Code 2010," *Structural Concrete*, vol. 14, no. 4, pp. 309–319, 2013.
[36] D. Straub and I. Papaioannou, "Bayesian updating with structural reliability methods," *Journal of Engineering Mechanics*, vol. 141, no. 3, 2015.
[37] H. Akaike, "A new look at the statistical model identification," *IEEE Transactions on Automatic Control*, vol. 19, no. 6, pp. 716–723, 1974.
[38] G. Schwarz, "Estimating the dimension of a model," *Annals of Statistics*, vol. 6, no. 2, pp. 461–464, 1978.
[39] S. Kullback and R. A. Leibler, "On information and sufficiency," *The Annals of Mathematical Statistics*, vol. 22, no. 1, pp. 79–86, 1951.
[40] D. J. C. MacKay, "Bayesian interpolation," *Neural Computation*, vol. 4, no. 3, pp. 415–447, 1992.
[41] H. Keitel, "Bewertungsmethoden für die Prognosequalität von Kriechmodellen des Betons; Evaluation Methods for Prediction Quality of Concrete Creep Models," Verlag der Bauhaus-Universität Weimar, Weimar, 2012, Ph.D. thesis.
[42] Q. A. Wang, Y. Dai, Z. Ma et al., "Towards probabilistic data-driven damage detection in SHM using sparse Bayesian learning scheme," *Structural Control and Health Monitoring*, vol. 29, no. 11, 2022.
[43] F. L. Zhang, C. W. Kim, and Y. Goi, "Efficient Bayesian FFT method for damage detection using ambient vibration data with consideration of uncertainty," *Structural Control and Health Monitoring*, vol. 28, no. 2, 2021.
[44] Deutsches Institut für Normung e.V., "Prüfverfahren; Referenzbetone für Prüfungen; Deutsche Fassung EN 1766:2000, DIN EN 1766, Deutsches Institut für Normung e.V," 2000.
[45] S. Pirskawetz, G. Hüsken, K.-P. Gründer, and D. Kadoke, "Damage mechanisms analysis of reinforced concrete beams in bending using non-destructive testing," in *Proceedings of the Sixth International Symposium on Life-Cycle Civil Engineering (IALCCE 2018)*, Ghent, Belgium, October 2019.
[46] F. McKenna, "OpenSees: a framework for earthquake engineering simulation," *Computing in Science and Engineering*, vol. 13, no. 4, pp. 58–66, 2011.
[47] M. Zhu, F. McKenna, and M. H. Scott, "OpenSeesPy: Python library for the OpenSees finite element framework," *SoftwareX*, vol. 7, pp. 6–11, 2018.
[48] S. N. Shoukry, G. W. William, B. Downie, and M. Y. Riad, "Effect of moisture and temperature on the mechanical properties of concrete," *Construction and Building Materials*, vol. 25, no. 2, pp. 688–696, 2011.

[49] Y. Jiao, H. Liu, X. Wang, Y. Zhang, G. Luo, and Y. Gong, "Temperature effect on mechanical properties and damage identification of concrete structure," *Advances in Materials Science and Engineering*, vol. 2014, Article ID 191360, 10 pages, 2014.
[50] G. Lee, T. Shih, and K.-C. Chang, "Mechanical properties of concrete at low temperature," *Journal of Cold Regions Engineering*, vol. 2, no. 1, pp. 13–24, 1988.
[51] A. Gelman, J. B. Carlin, H. S. Stern, D. B. Dunson, A. Vehtari, and D. B. Rubin, "Bayesian data analysis," *Chapman and Hall/CRC Texts in Statistical Science*, CRC Press, Boca Raton, 2014.
[52] K.-V. Yuen and L. Dong, "Real-time system identification using hierarchical interhealing model classes," *Structural Control and Health Monitoring*, vol. 27, no. 12, p. e2628, 2020.
[53] P. Simon, R. Schneider, M. Baeßler, and G. Morgenthal, "Parallelized adaptive Bayesian Updating with Structural reliability methods for inference of large engineering models (manuscript submitted for review in Advances in Structural Engineering)," 2024.
[54] A. Kamariotis and E. Chatzi, "Bayesian decision-theoretic model selection for monitored systems," 2023, https://arxiv.org/abs/2310.10485.